Supplementary Information for

Systematic Profiling of Essential Fungal Transcription Factors Uncovers Ezt1 as a Central Pathobiological and Morphogenic Regulator in *Cryptococcus neoformans*

Seung-Heon Lee[1†], Sheng Sun[2], Yu-Byeong Jang[1], Seong-Ryong Yu[1], Yeseul Choi[2], Jin-Tae Choi[1], Eui-Seong Kim[3], Jong-Seung Lee[4], Joseph Heitman[2*], Kyung-Tae Lee[3 *], and Yong-Sun Bahn[1*]

[1]Department of Biotechnology, College of Life Science and Biotechnology, Yonsei University, Seoul 03722, Republic of Korea

[2]Department of Molecular Genetics and Microbiology, Duke University Medical Center, Durham, NC27710, USA

[3]Korea Zoonosis Research Institute, Jeonbuk National University, Iksan, Jeonbuk State 54531, Republic of Korea

[4]AmtixBio Co., Ltd., Seoul 05836, Republic of Korea

This PDF file includes:

Supplementary Table 1

Supplementary Figures 1 – 14

Supplementary Table 1. Essentiality of the 17 putative essential TFs.

Name	TF Family	Nomenclature	Essentiality in other model fungus	Functional annotations in FungiDB	Growth of P_{CTR4}	CnLC6683		AI187				Essentiality in *C. neoformans*
						Spore dissection		Spore dissection		Spore separation		
						Total	KO	Total	KO	Total	KO	
CEF1	Myb	Named after close orthologue in *S. cerevisiae*	*S. cerevisiae* *S. pombe* *N. glabratus*	Pre-mRNA-splicing factor Cef1	Required	44	0	Not executed				Essential
SNU66	SART1	Named after close orthologue in *S. cerevisiae*	*S. pombe* *C. albicans*	U4/U6.U5 tri-snRNP-associated protein 1	Required	48	0	N/A		31	0	Essential
EAT1	APSES	Named as essential APSES TF 1	-	Hypothetical protein	Required	45	0	N/A		55	0	Essential
CDC39	Ccr4-Not1 Complex	Named after close orthologue in *S. cerevisiae*	*S. pombe* *N. glabratus*	CCR4-NOT transcription complex subunit 1	Required	20	0	2	0	77	0	Essential
EZT2	Zn2Cys6	Named as essential zinc finger TF 2	-	Hypothetical protein	Required	56	0	56	0	10	0	Essential
ZAP101	C2H2 Zinc Finger	Named based on distant homology to *S. cerevisiae ZAP1*	-	Zinc finger protein	Required	39	0	7	0	21	0	Essential
RSC8	Myb	Previously annotated in FungiDB	*S. cerevisiae* *S. pombe* *C. albicans*	RSC chromatin remodeling complex subunit	Weakly required	46	0	N/A		33	0	Essential
PZF1	C2H2 Zinc Finger	Named after close orthologue in *S. cerevisiae*	*S. cerevisiae* *S. pombe* *N. glabratus*	Transcription factor IIIA	Weakly required	15	0	46	0	N/A		Essential
ESA1	Winged helix repressor DNA-binding	Named after close orthologue in *S. cerevisiae*	*S. cerevisiae* *S. pombe* *N. glabratus*	Histone acetyltransferase Esa1	Weakly required	56	0	N/A		55	0	Essential
EZT1	Zn2Cys6	Named after TF family classification	-	Hypothetical protein	Weakly required	21	0	N/A		29	0	Essential
FHL1	Winged helix repressor DNA-binding	Named as essential zinc finger TF 1	*N. glabratus*	Pre-rRNA-processing protein Fhl1, putative	Weakly required	46	13	N/A		68	0	Quasi-essential
CBF1	bHLH	Named based on predicted protein domain	-	Hypothetical protein	Weakly required	Not executed		17	0	61	0	Essential
TOP3	Zinc Finger, GRF-type	Named after close orthologue in *S. cerevisiae*	*S. pombe* *N. glabratus*	DNA topoisomerase III	Weakly required	Not executed		N/A		33	0	Essential
SGT1	SGT1	Named based on predicted protein domain	*S. pombe*	Hypothetical protein	Weakly required	77	0	11	0	41	0	Essential
HLH7	Helix-turn-helix, Psq	Named after TF family classification	-	Hypothetical protein	Non-required	42	19	3	0	41	0	Non-essential
ASR2	-	Named based on predicted protein domain	*S. pombe*	Arsenite-resistant protein Asr2	Non-required	85	35	10	0	84	0	Non-essential
FZC52	Zn2Cys6	Named after TF family classification	-	Hypothetical protein	Non-required	80	30	Not executed				Non-essential

Supplementary Table 1 includes information on essentiality in other species based on BLAST results, FungiDB annotations, and contributions to fungal growth inferred from conditional expression regulation. Additionally, heterozygous mutants generated in this study were utilised to determine the essentiality through meiotic spore analysis, with the number of the spores and knock-out progeny included. Abbreviations: N/A, not-analysable due to defective sporulation; KO, knockout; Quasi-essential, growth-required but non-essential.

Supplementary figure 1 (Lee et al.)

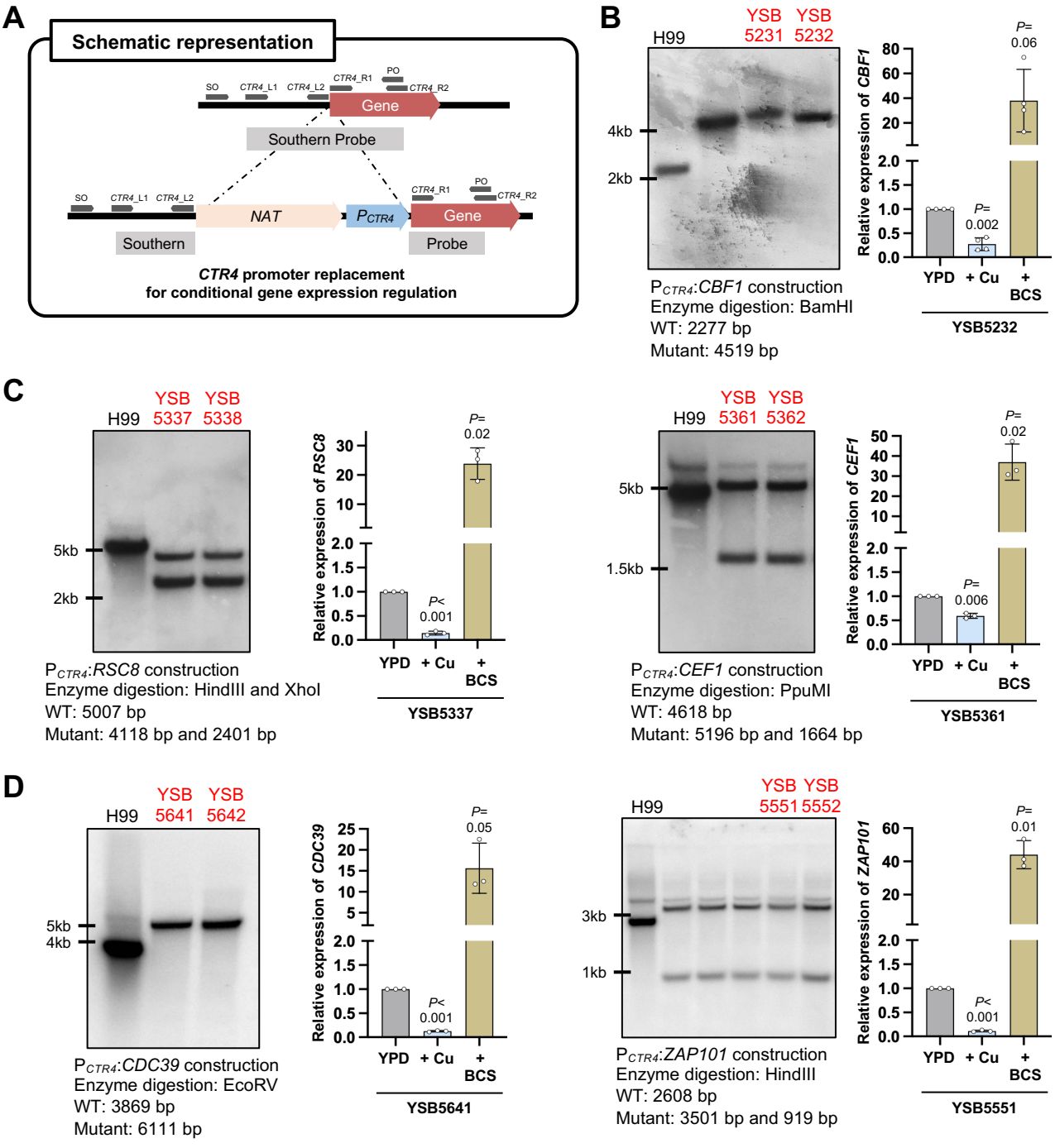

Continued

E

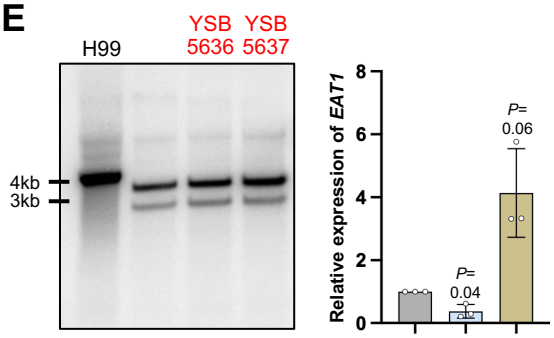

P_{CTR4}:*EAT1* construction
Enzyme digestion: PpuMI
WT: 4196 bp
Mutant: 3579 bp and 2859 bp

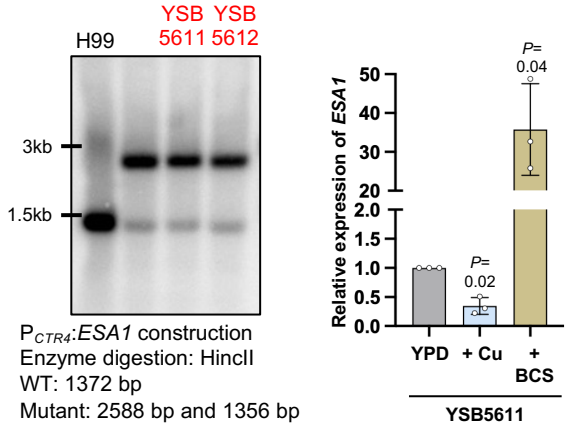

P_{CTR4}:*ESA1* construction
Enzyme digestion: HincII
WT: 1372 bp
Mutant: 2588 bp and 1356 bp

F

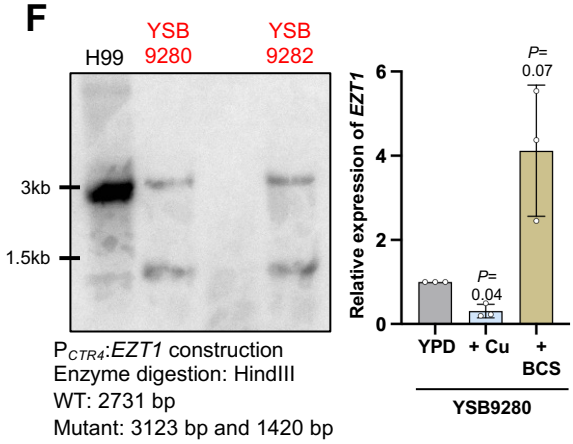

P_{CTR4}:*EZT1* construction
Enzyme digestion: HindIII
WT: 2731 bp
Mutant: 3123 bp and 1420 bp

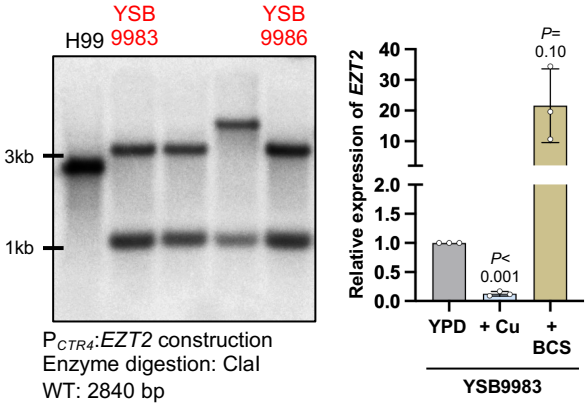

P_{CTR4}:*EZT2* construction
Enzyme digestion: ClaI
WT: 2840 bp
Mutant: 3693 bp and 1168 bp

G

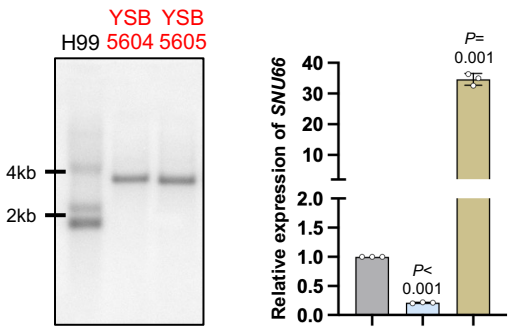

P_{CTR4}:*SNU66* construction
Enzyme digestion: BglIII
WT: 1957 bp
Mutant: 3938 bp

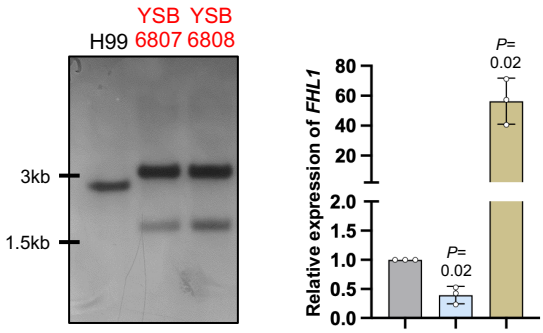

P_{CTR4}:*FHL1* construction
Enzyme digestion: EcoRI
WT: 2823 bp
Mutant: 3272 bp and 1793 bp

Continued

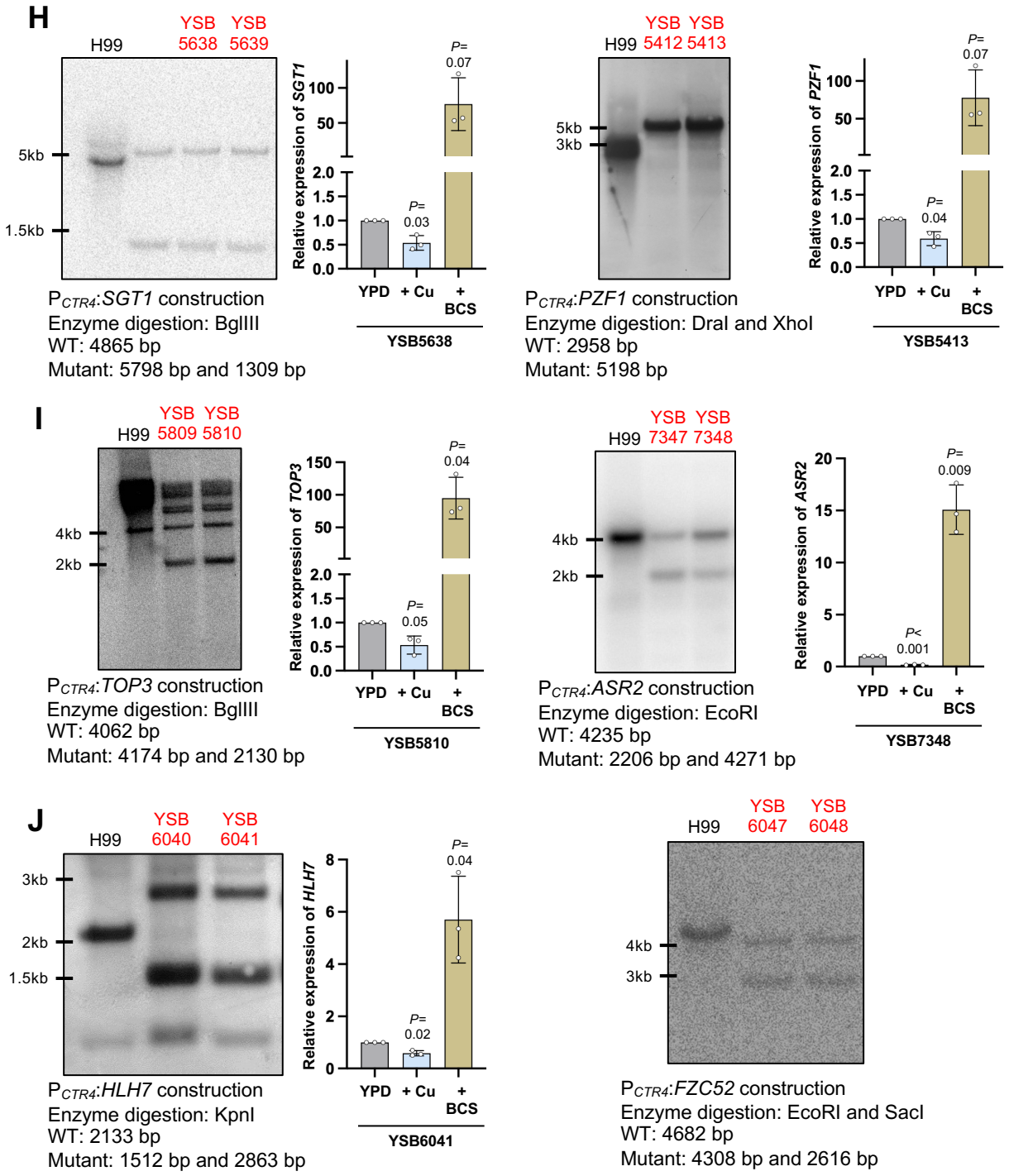

Supplementary figure 1. Construction of the *CTR4* promoter replacement strains. (A) Schematic representation for the construction of the conditionally regulatable strains. (B - J) Correct genotypes of the strains were confirmed through Southern blot analysis with the designated restriction enzyme digestion of genomic DNA and gene-specific probes. The regulation of the targeted genes was confirmed with quantitative reverse transcription-PCR (qRT-PCR). The strains were grown overnight at 30°C in 2 ml of liquid YPD medium (OD_{600nm}=0.2), subcultured into 10 ml of fresh YPD medium, YPD + 40 μM $CuSO_4$, and 200 μM BCS (bathocuproinedisulphonic acid) respectively. Cell cultures were further incubated at 30°C in a shaking incubator for eight hours, harvested, and frozen in liquid nitrogen and lyophilized. Total RNAs were isolated using easy-BLUE™ total RNA extraction kit (iNtRON biotechnology, Republic of Korea), and cDNAs were synthesized using Maxima H minus reverse transcriptase followed by the manufacturer's protocol (Thermo Fisher Scientific, USA). qRT-PCRs were performed using gene-specific primer pairs, and the expression levels of the genes were normalized with *ACT1* expression. Data are represented as mean ± SD (standard deviation). Statistical significance of difference of repression and induction was determined by one-sample *t*-test with YPD conditions (=1) using Prism 11.0 (*P* values are indicated above the bar graph).

Supplementary figure 2 (Lee et al.)

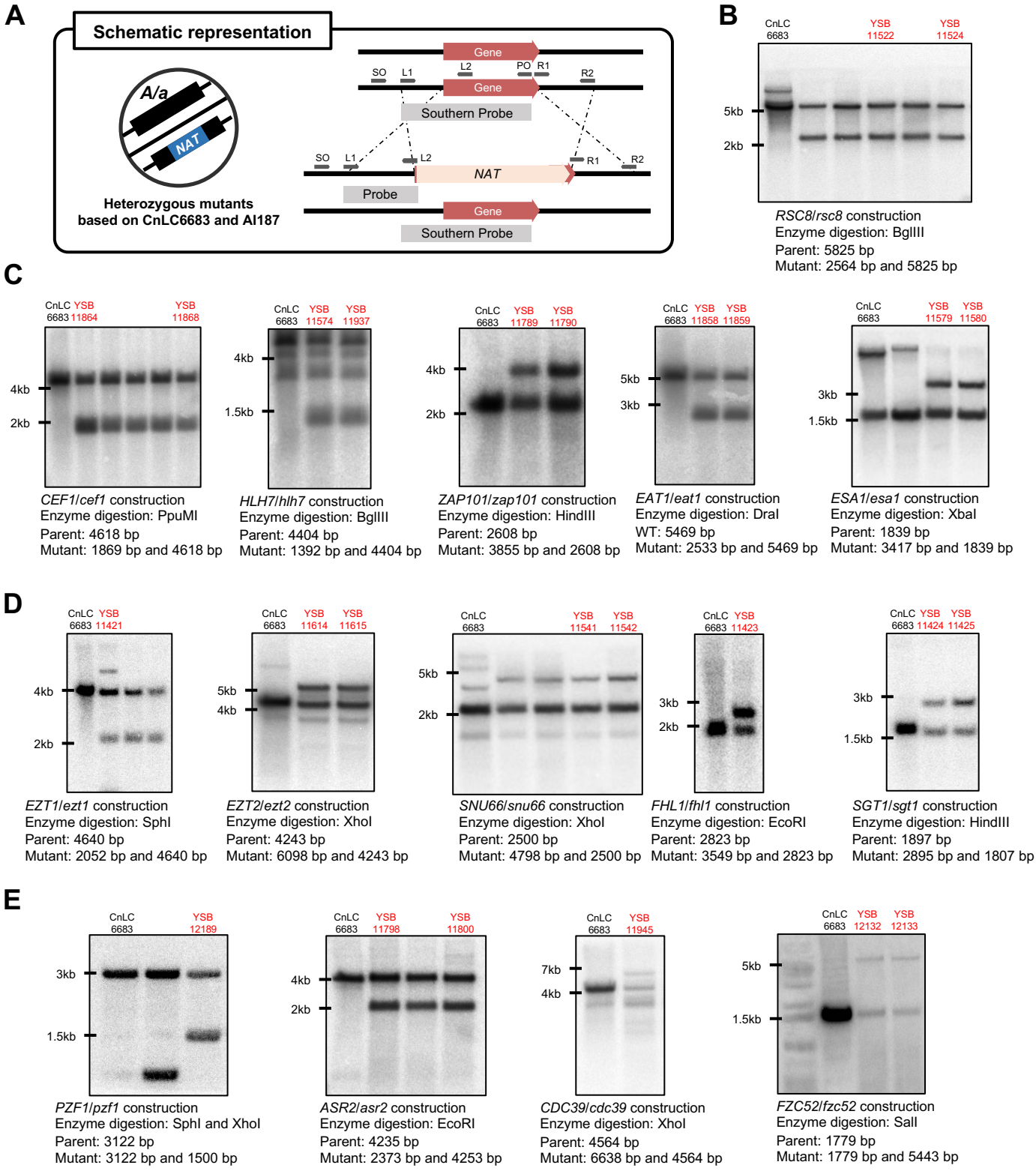

Supplementary figure 2. Construction of the heterozygous mutants based on diploid CnLC6683. (A) Schematic representation for the construction of the heterozygous mutant strains in the genetically engineered diploid CnLC6683 strain. (B-E) Correct genotypes of the heterozygous mutant strains were confirmed through Southern blot analysis with the designated restriction enzyme digestion of genomic DNA and gene-specific probes.

Supplementary Figure 3 (Lee et al.)

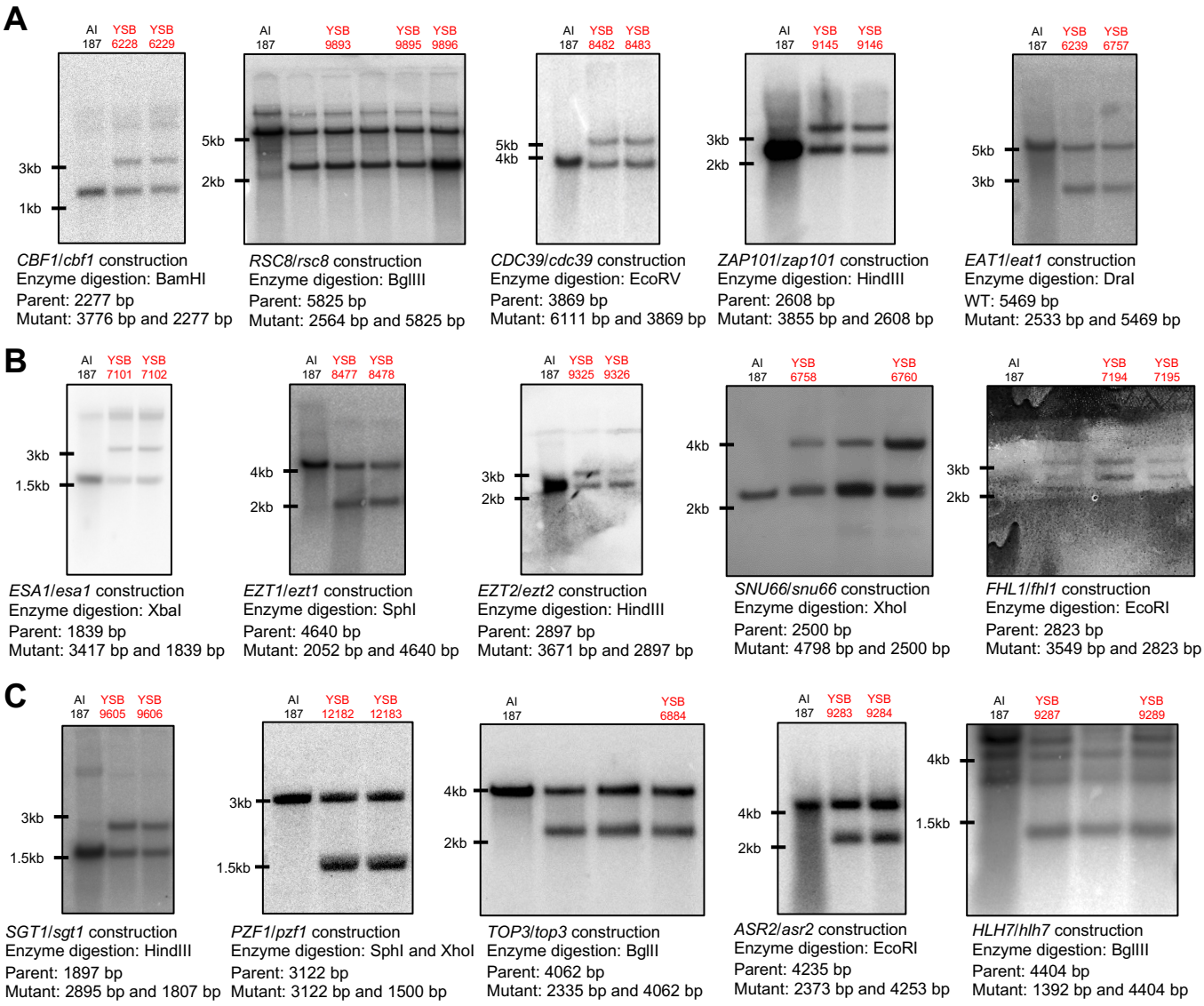

Supplementary figure 3. Construction of the heterozygous mutants based on diploid AI187. Schematic representation for the construction of the heterozygous mutant strains in the diploid AI187 strain is shown in the supplementary figure 2A. (A-C) Correct genotypes of the heterozygous mutant strains were confirmed through Southern blot analysis with the designated restriction enzyme digestion of genomic DNA and gene-specific probes.

Supplementary Figure 4 (Lee et al.)

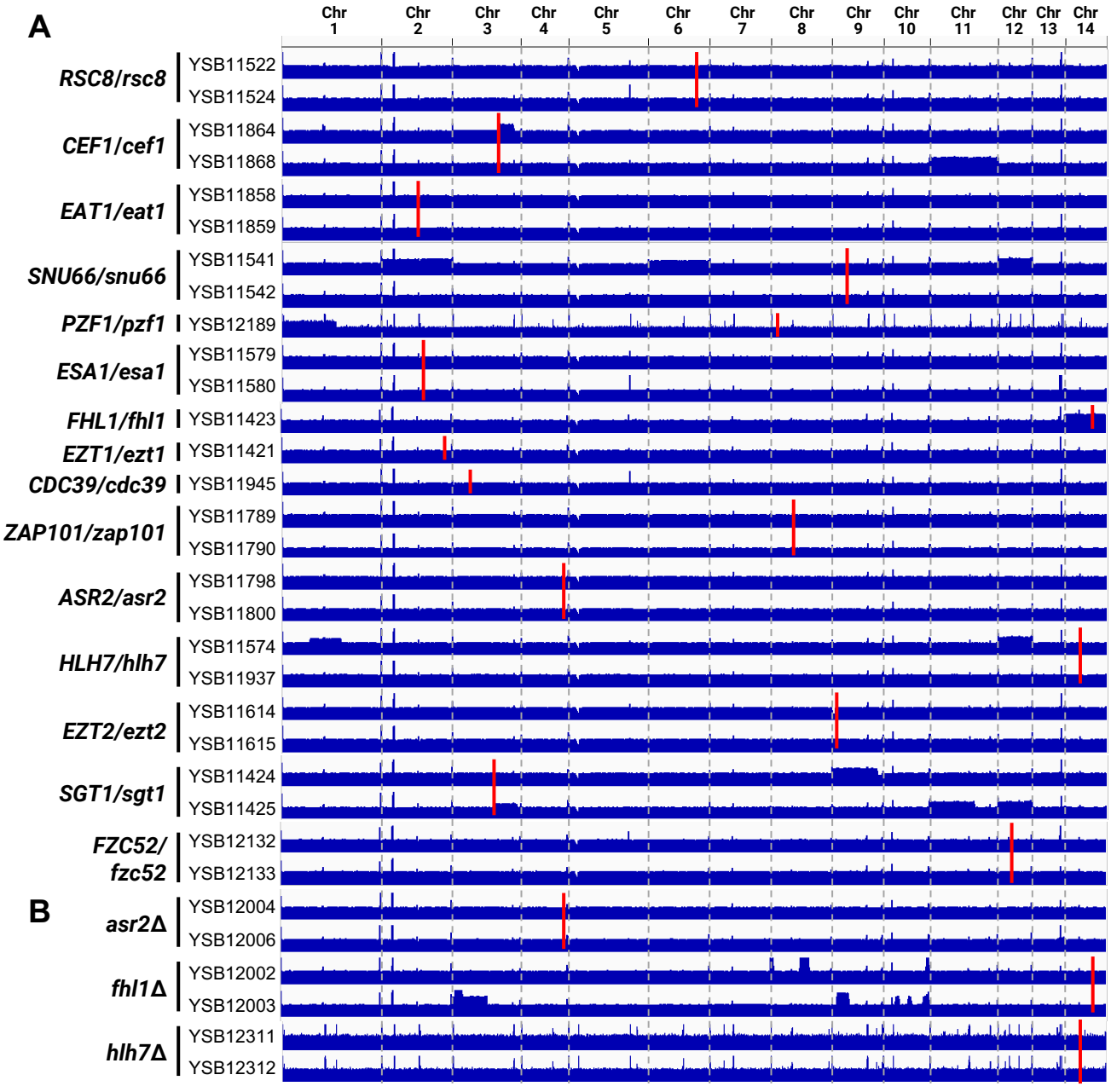

Continued

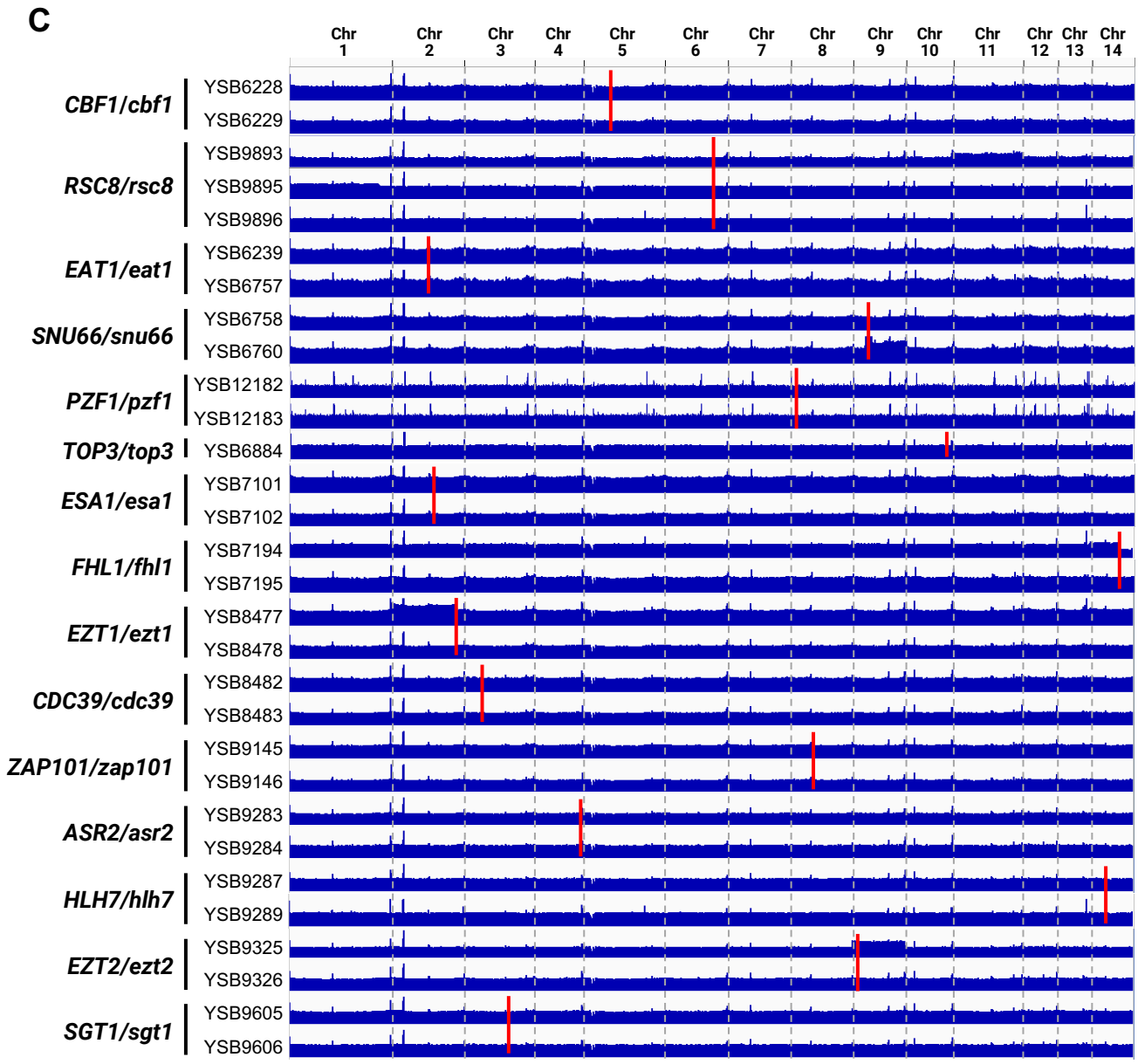

Supplementary figure 4. Whole-genome sequencing (WGS) coverage plots of (A) heterozygous mutants generated in the CnLC6683 background, (B) knockout progenies derived from the CnLC6683-based heterozygous mutants, and (C) heterozygous mutants constructed in the AI187 background. Genomic DNA extracted from each strain was subjected to Illumina sequencing, followed by read alignment to the *Cryptococcus neoformans* H99 reference genome using BWA. Alignment files were processed and converted using SAMtools, and genome-wide coverage depth was calculated using a binning size of 100 base pairs. Resulting coverage profiles were visualised using IGV to assess genome integrity, chromosomal CNV patterns, and potential structural variations across strains. In each coverage plot, the chromosomal positions of genes targeted are marked by red bars.

Supplementary Figure 5 (Lee et al.)

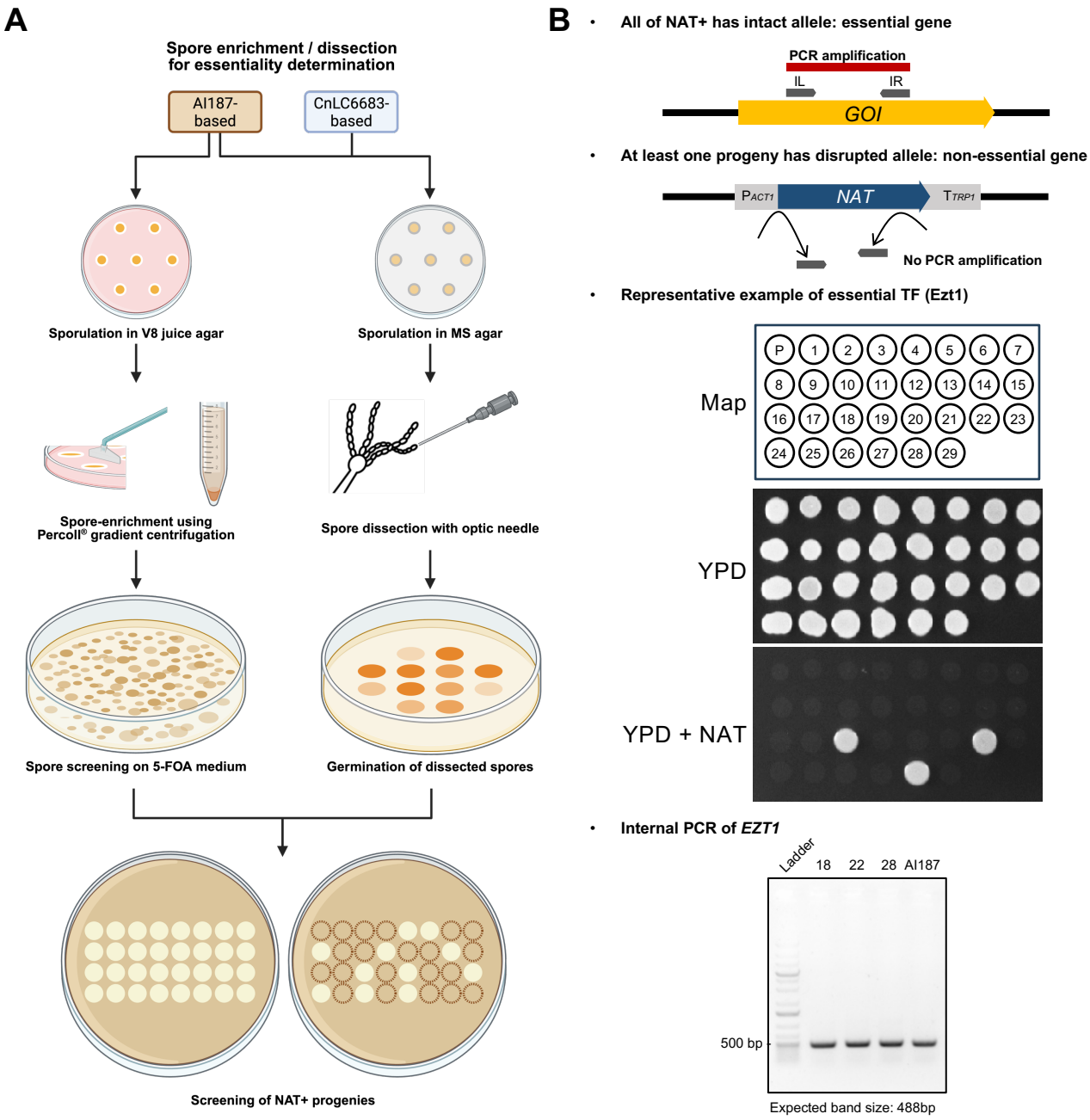

Supplementary figure 5. Schematic overview and representative example of meiotic pore analysis following spore separation and dissection. (A) Schematic overview of the spore analysis workflow. Heterozygous mutants generated in the diploid strain AI187 were subjected to spore separation by gradient centrifugation and spore dissection using a micromanipulation needle. Heterozygous mutants generated in the diploid strain CnLC6683 were subjected only to spore dissection because the parental strain lacks auxotrophic markers. After progeny identification by *MAT* locus PCR, progenies were further validated for the presence of the drug resistance marker by spotting on YPD plate containing nourseothricin. The illustration was created with Biorender. (B) Representative example of essentiality validation for *EZT1*. Internal PCR was performed on nourseothricin resistant progeny using the primer pari B6117 and B14784, which anneal within the deletion target region. All essential TFs were validated using the same method shown here.

Supplementary figure 6 (Lee et al.)

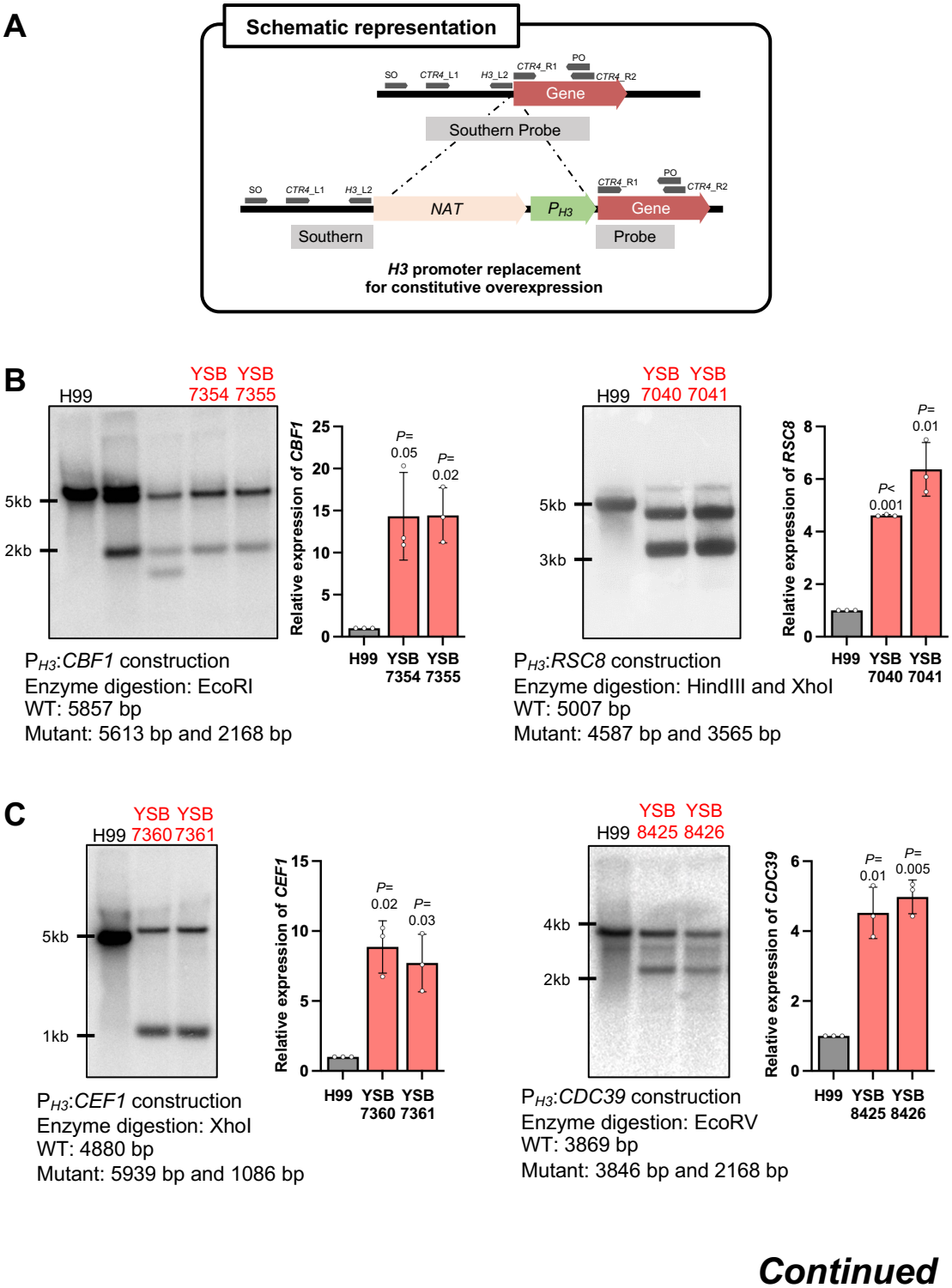

Continued

D

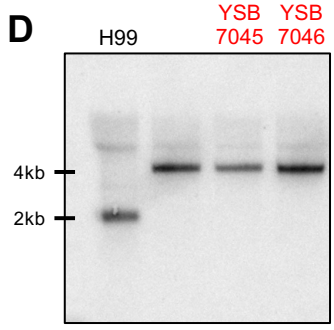

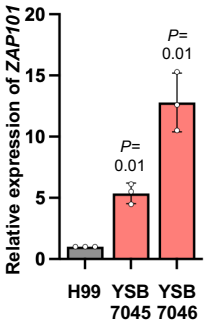

P_{H3}:*ZAP101* construction
Enzyme digestion: DraI
WT: 2137 bp
Mutant: 4282 bp

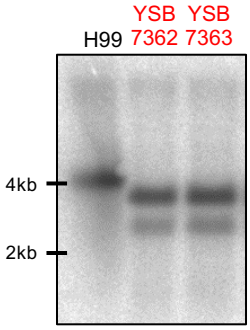

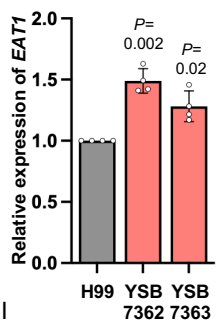

P_{H3}:*EAT1* construction
Enzyme digestion: PpuMI
WT: 4196 bp
Mutant: 3581 bp and 2760 bp

E

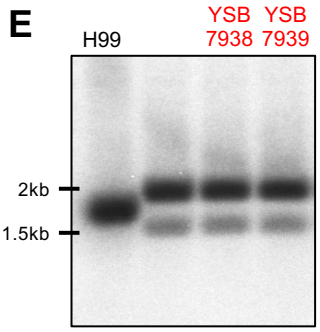

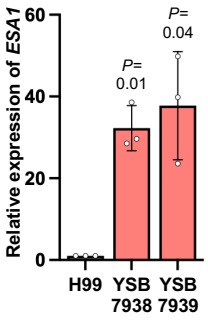

P_{H3}:*ESA1* construction
Enzyme digestion: EcoRI
WT: 1840 bp
Mutant: 2186 bp and 1578 bp

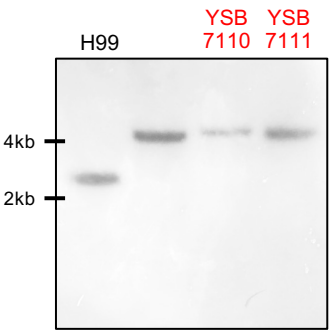

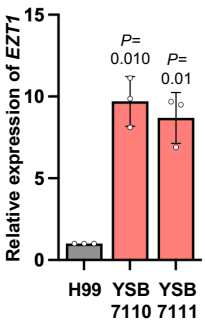

P_{H3}:*EZT1* construction
Enzyme digestion: HindIII
WT: 2731 bp
Mutant: 4876 bp

F

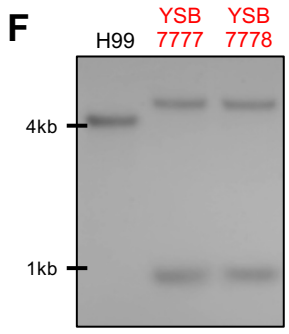

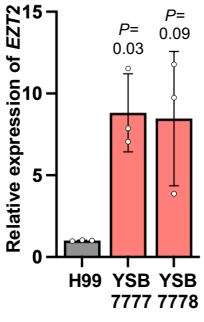

P_{H3}:*EZT2* construction
Enzyme digestion: XhoI
WT: 4243 bp
Mutant: 5415 bp and 973 bp

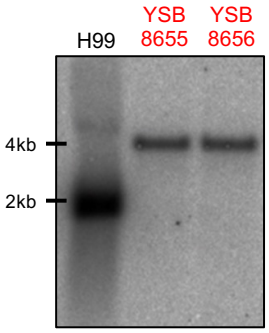

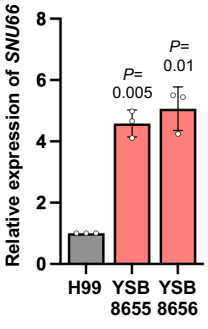

P_{H3}:*SNU66* construction
Enzyme digestion: BglIII
WT: 1957 bp
Mutant: 4102 bp

Continued

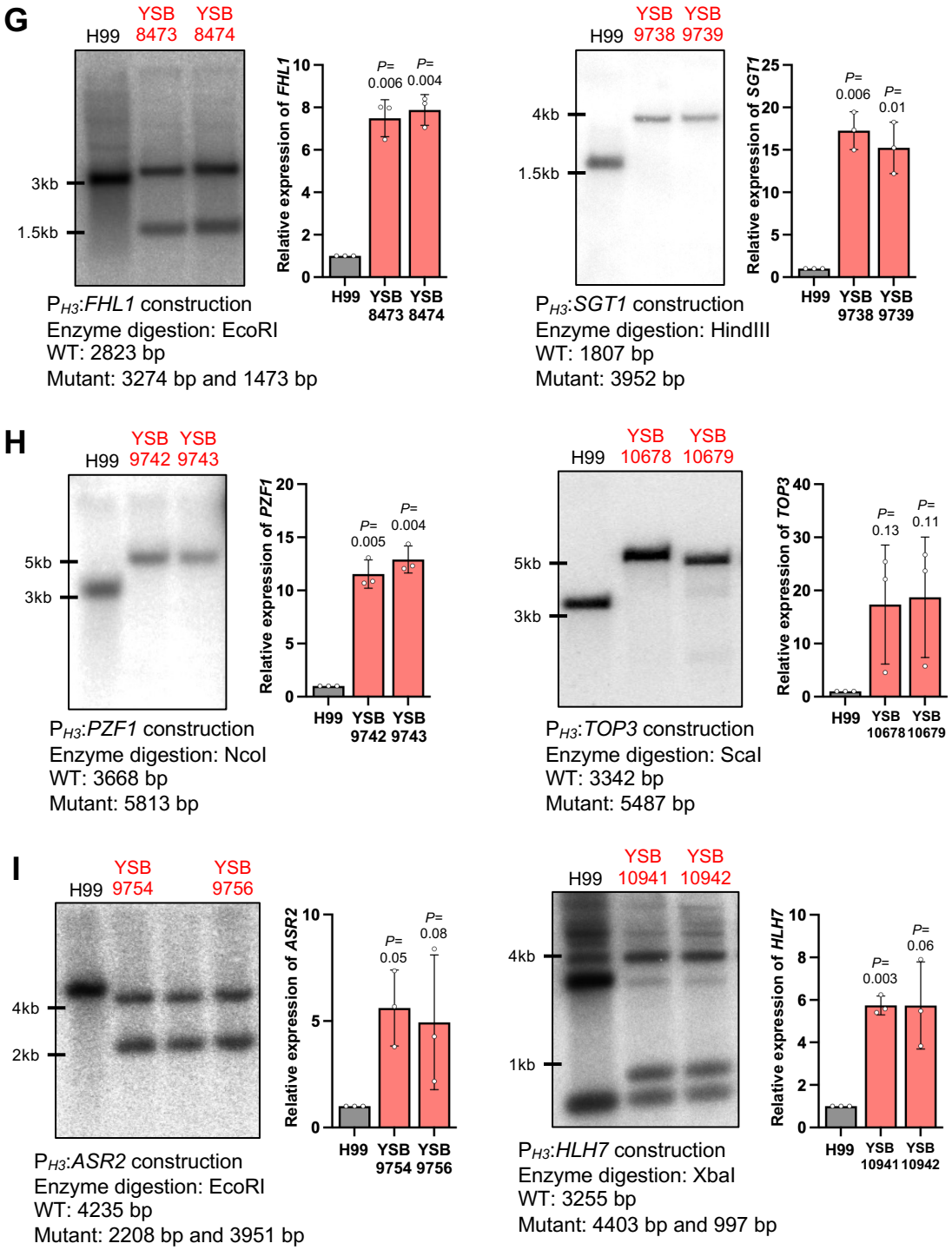

Supplementary figure 6. Construction of the constitutive overexpression strains. (A) Schematic representation for the construction of the histone 3 (H3) promoter-derived constitutive overexpression strains. (B-I) Correct genotypes of each overexpression strain were confirmed through Southern blot analysis with the designated restriction enzyme digestion of genomic DNA and gene-specific probes. The overexpression of the targeted genes was confirmed with qRT-PCR. The strains were grown overnight at 30°C in 50 ml of liquid YPD medium, subcultured into 50 ml of fresh YPD medium (OD_{600nm}=0.2). Cell cultures were further incubated at 30°C in a shaking incubator until OD600nm reaches between 0.6 and 0.8, harvested, frozen in liquid nitrogen, and lyophilized. Total RNAs were isolated, and cDNAs were synthesized. qRT-PCRs were performed using gene-specific primer pairs and the expression levels of the genes were normalized with *ACT1* expression. Data are represented as mean ± SD. Statistical significance of difference between wild-type and the overexpression strain was determined by one-sample *t*-test using Prism 11.0 (*P* values are indicated above the bar graph).

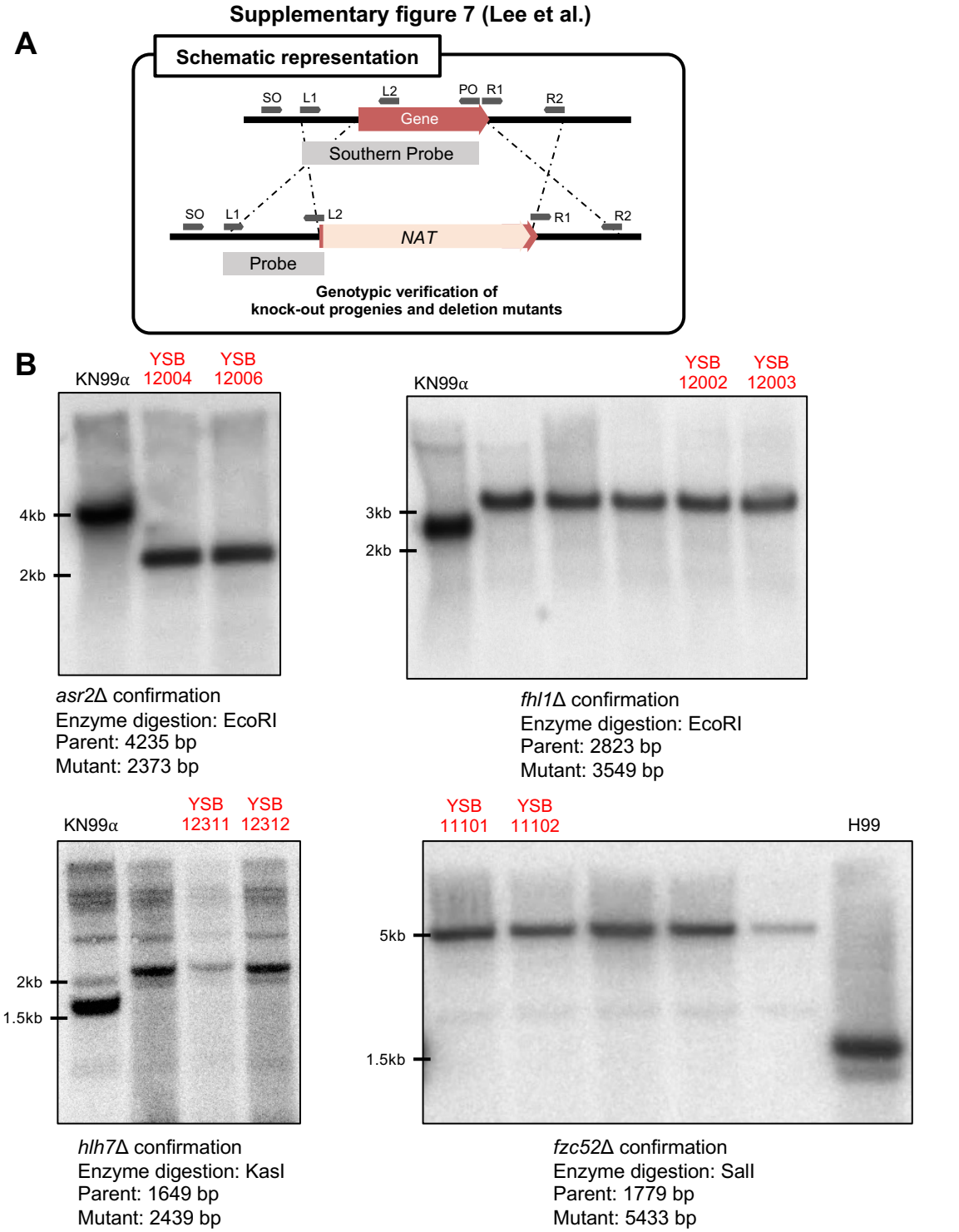

Supplementary figure 7. Confirmation of the deletion mutants of non-essential TFs (*ASR2*, *FHL1*, and *FZC52*). (A) Schematic representation for confirming the haploid knockout strains. (B) The genomic DNA of wild-type (KN99 for *asr2*Δ spores and *fhl1*Δ spores, and H99 for *fzc52*Δ) knock-out haploid spores and mutants were subjected to restriction enzyme digestion and proceeded to Southern blot analysis with the gene-specific probes.

Supplementary figure 8 (Lee et al.)

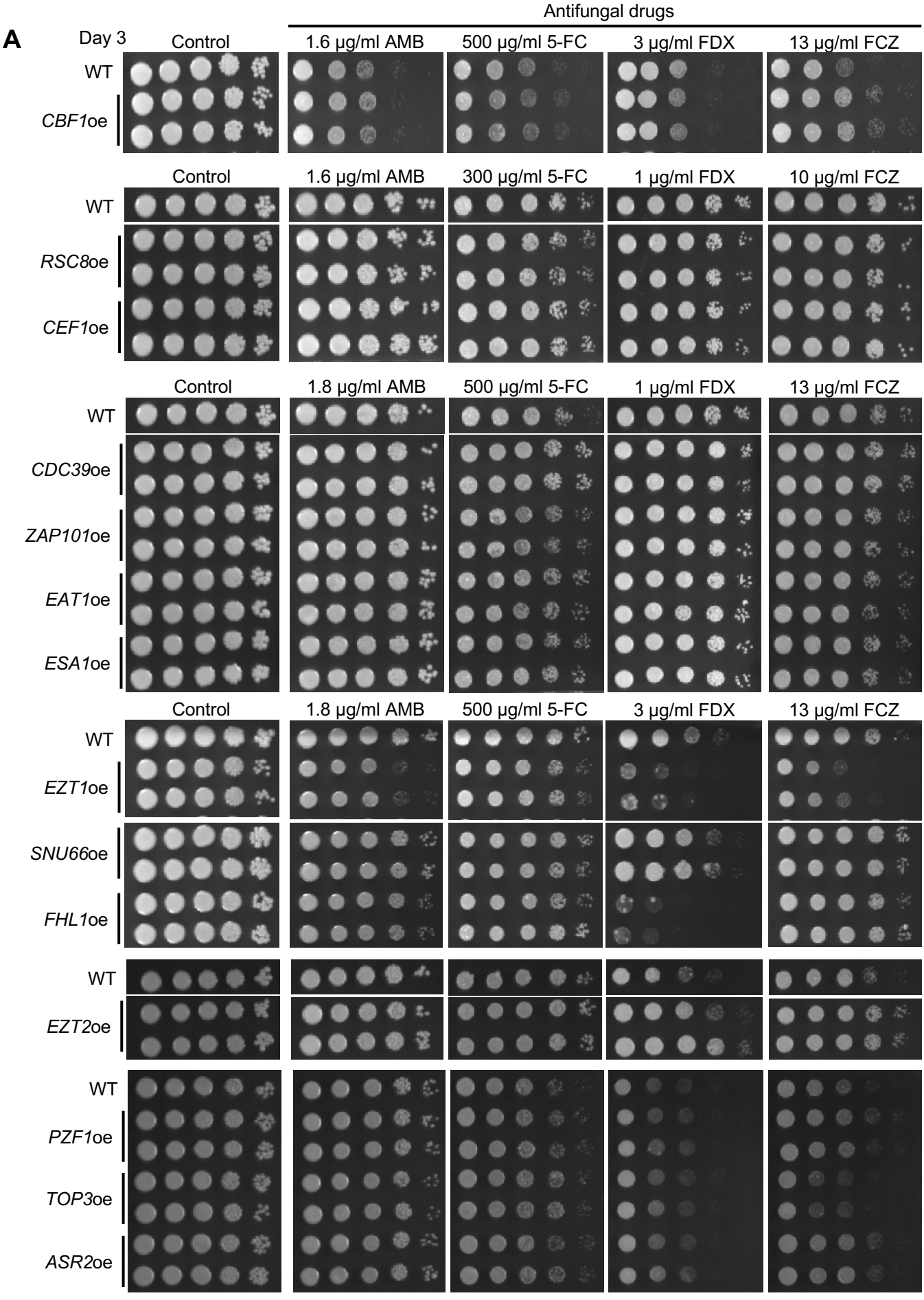

Continued

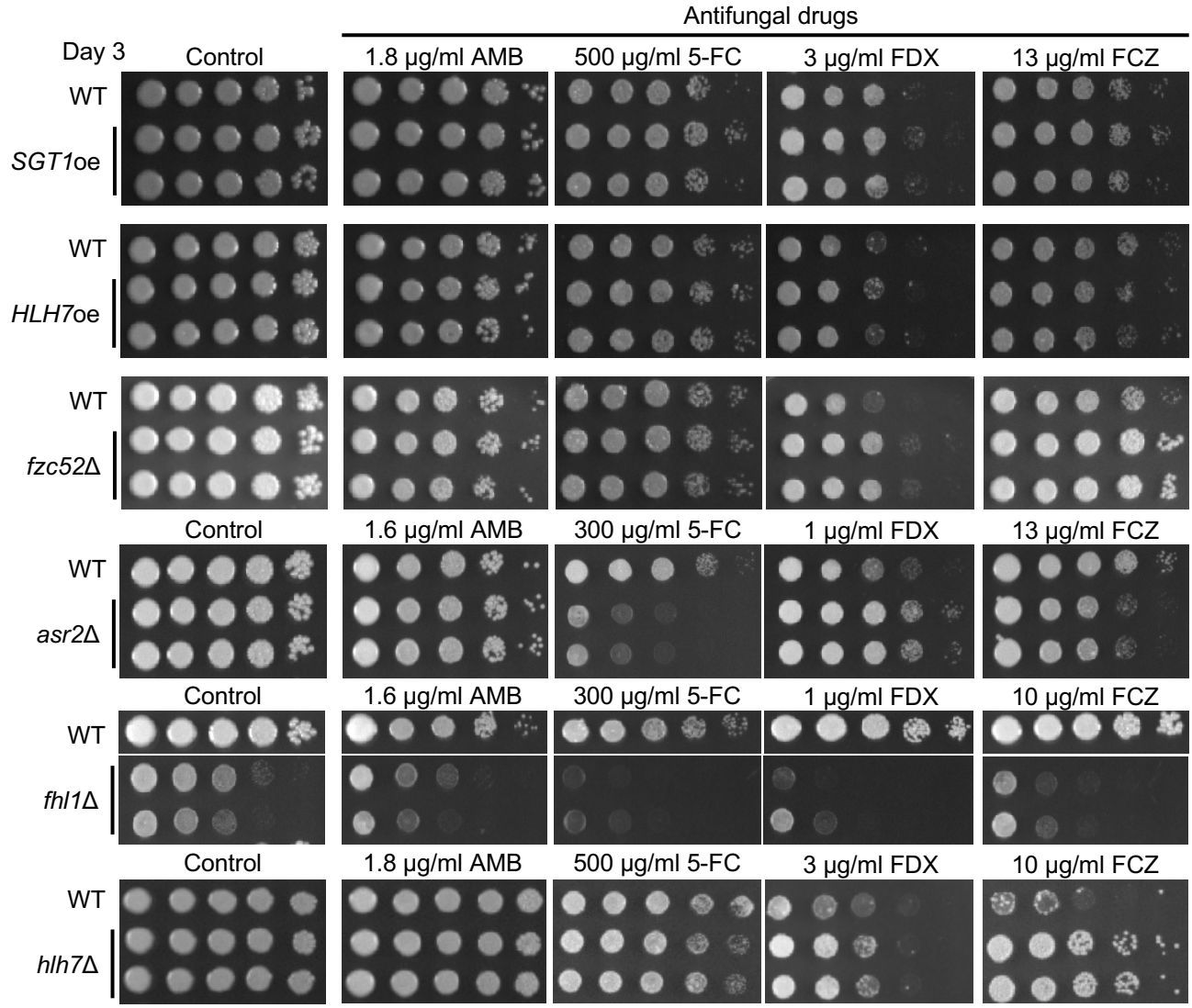
Antifungal drugs
Day 3
Control
1.8 μg/ml AMB
500 μg/ml 5-FC
3 μg/ml FDX
13 μg/ml FCZ
WT
SGT1oe
WT
HLH7oe
WT
fzc52Δ
Control
1.6 μg/ml AMB
300 μg/ml 5-FC
1 μg/ml FDX
13 μg/ml FCZ
WT
asr2Δ
Control
1.6 μg/ml AMB
300 μg/ml 5-FC
1 μg/ml FDX
10 μg/ml FCZ
WT
fhl1Δ
Control
1.8 μg/ml AMB
500 μg/ml 5-FC
3 μg/ml FDX
10 μg/ml FCZ
WT
hlh7Δ

B

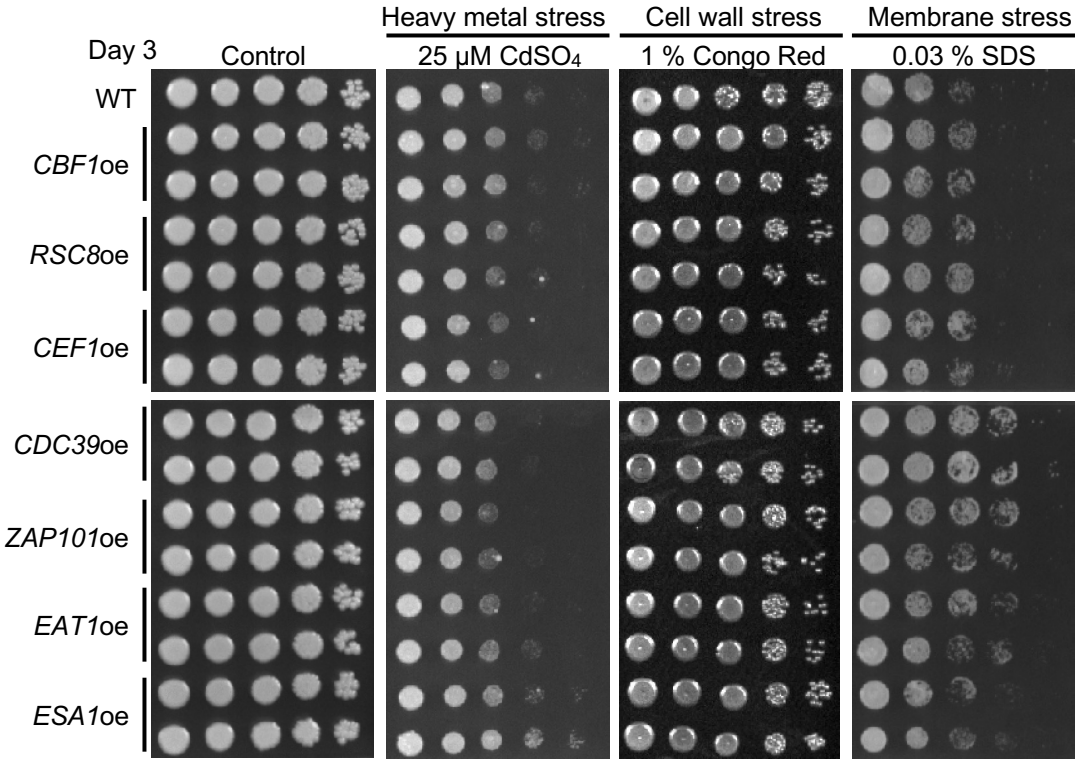
Heavy metal stress
Cell wall stress
Membrane stress
Day 3
Control
25 μM CdSO4
1 % Congo Red
0.03 % SDS
WT
CBF1oe
RSC8oe
CEF1oe
CDC39oe
ZAP101oe
EAT1oe
ESA1oe

Continued

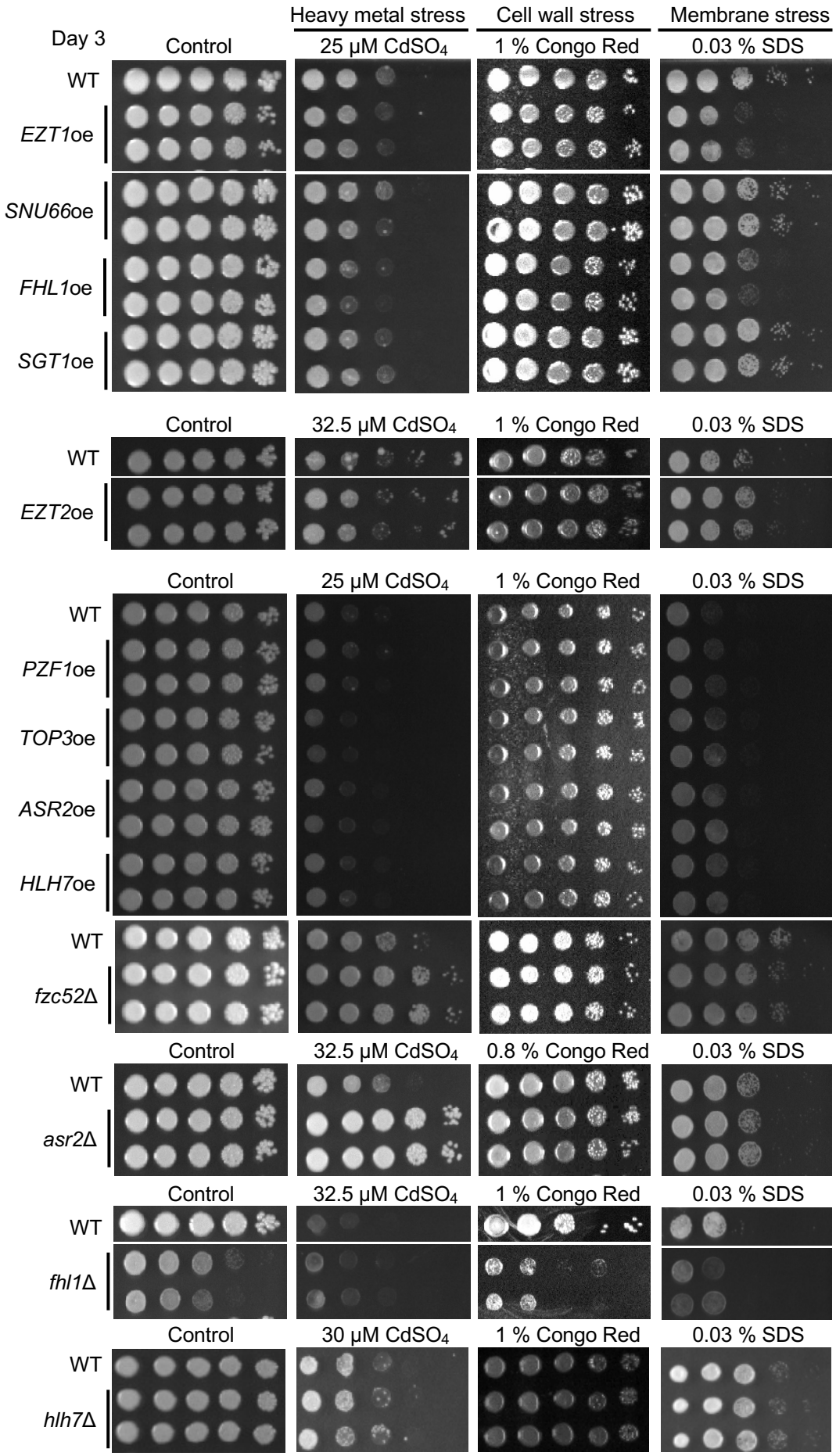
Heavy metal stress
Cell wall stress
Membrane stress
Day 3
Control
25 μM CdSO4
1 % Congo Red
0.03 % SDS
WT
EZT1oe
SNU66oe
FHL1oe
SGT1oe
Control
32.5 μM CdSO4
1 % Congo Red
0.03 % SDS
WT
EZT2oe
Control
25 μM CdSO4
1 % Congo Red
0.03 % SDS
WT
PZF1oe
TOP3oe
ASR2oe
HLH7oe
WT
fzc52Δ
Control
32.5 μM CdSO4
0.8 % Congo Red
0.03 % SDS
WT
asr2Δ
Control
32.5 μM CdSO4
1 % Congo Red
0.03 % SDS
WT
fhl1Δ
Control
30 μM CdSO4
1 % Congo Red
0.03 % SDS
WT
hlh7Δ

Continued

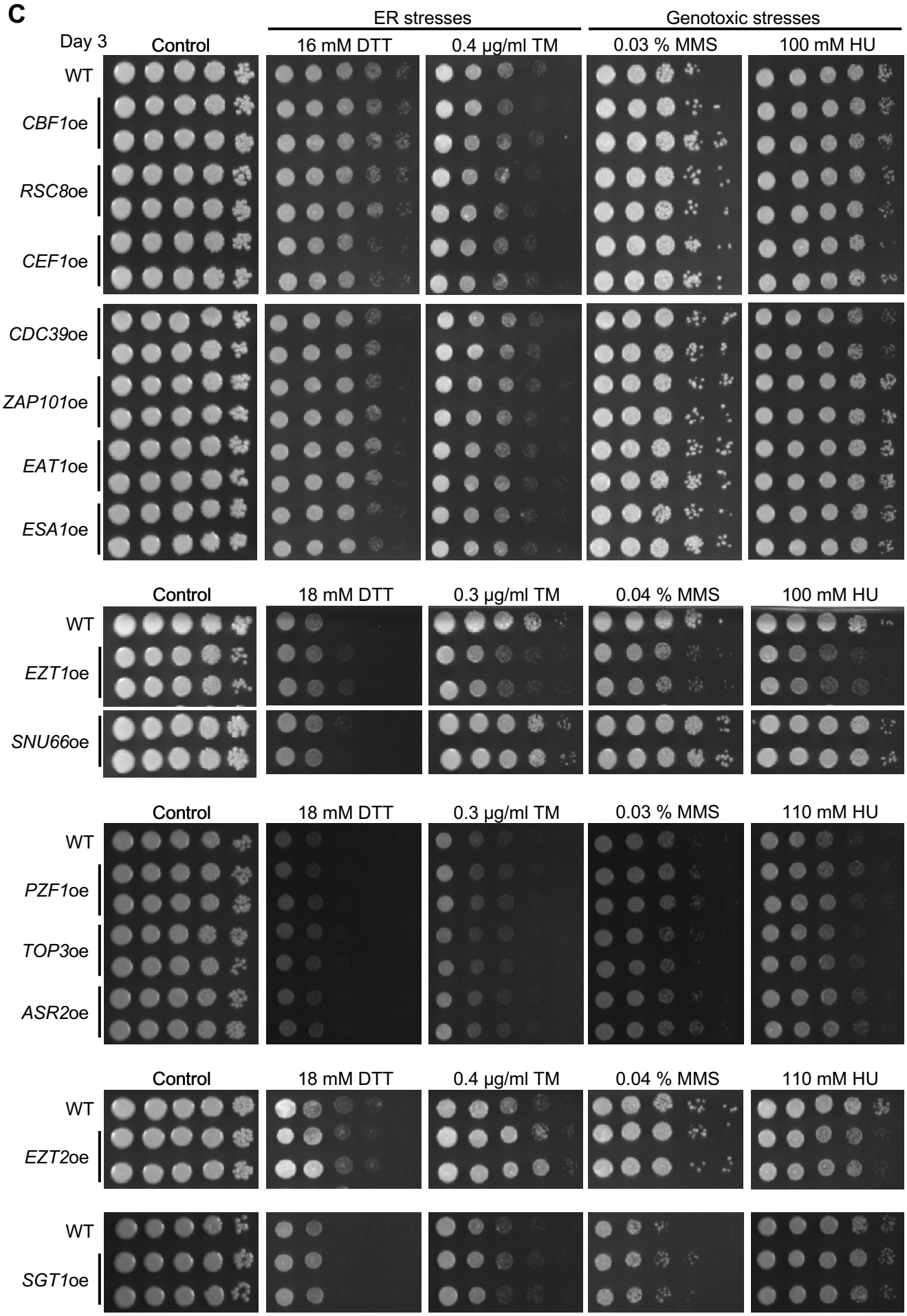
C
ER stresses
Genotoxic stresses
Day 3
Control
16 mM DTT
0.4 μg/ml TM
0.03 % MMS
100 mM HU
WT
CBF1oe
RSC8oe
CEF1oe
CDC39oe
ZAP101oe
EAT1oe
ESA1oe
Control
18 mM DTT
0.3 μg/ml TM
0.04 % MMS
100 mM HU
WT
EZT1oe
SNU66oe
Control
18 mM DTT
0.3 μg/ml TM
0.03 % MMS
110 mM HU
WT
PZF1oe
TOP3oe
ASR2oe
Control
18 mM DTT
0.4 μg/ml TM
0.04 % MMS
110 mM HU
WT
EZT2oe
WT
SGT1oe

Continued

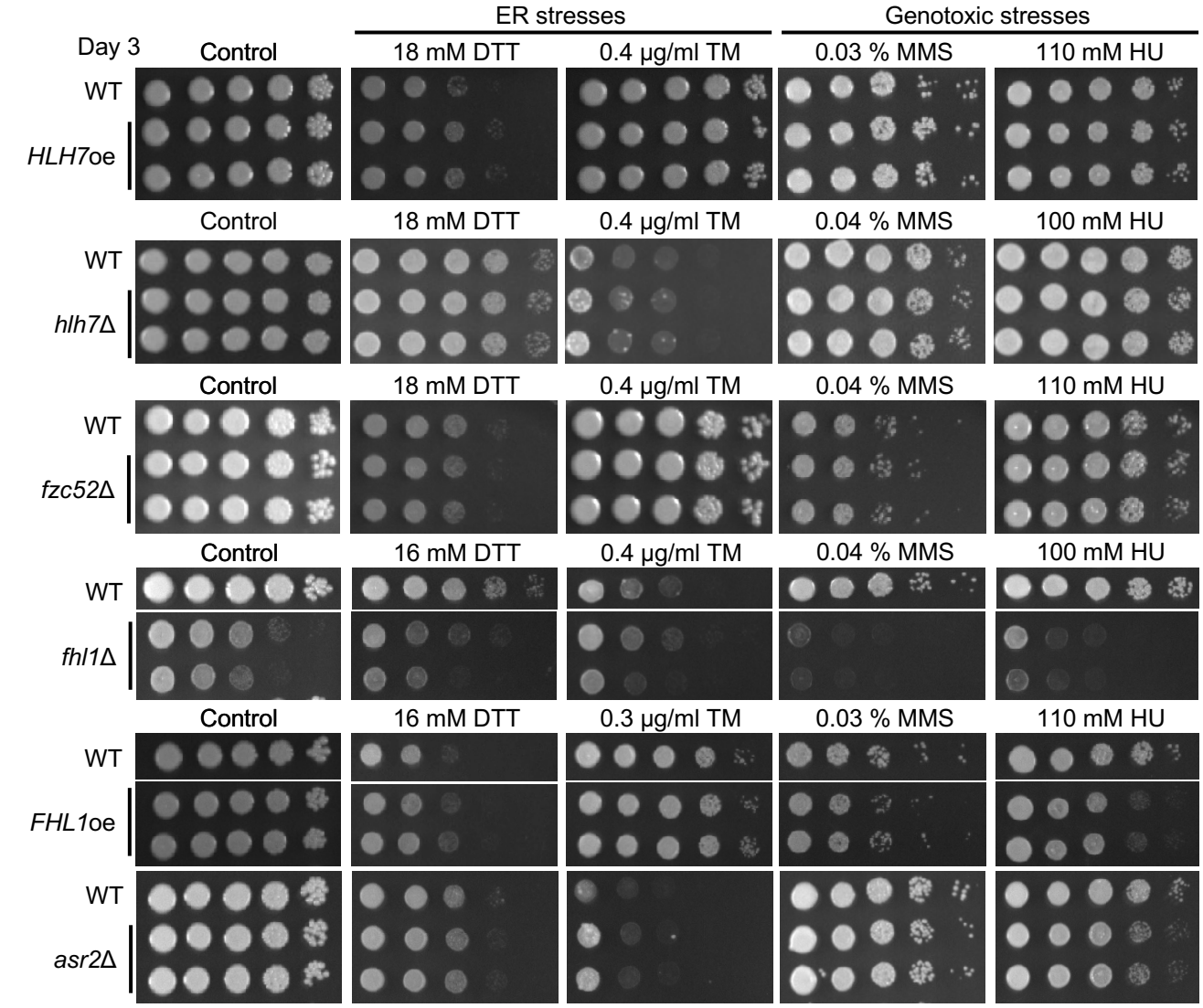
ER stresses
Genotoxic stresses
Day 3
Control
18 mM DTT
0.4 μg/ml TM
0.03 % MMS
110 mM HU
WT
HLH7oe
Control
18 mM DTT
0.4 μg/ml TM
0.04 % MMS
100 mM HU
WT
hlh7Δ
Control
18 mM DTT
0.4 μg/ml TM
0.04 % MMS
110 mM HU
WT
fzc52Δ
Control
16 mM DTT
0.4 μg/ml TM
0.04 % MMS
100 mM HU
WT
fhl1Δ
Control
16 mM DTT
0.3 μg/ml TM
0.03 % MMS
110 mM HU
WT
FHL1oe
WT
asr2Δ

D

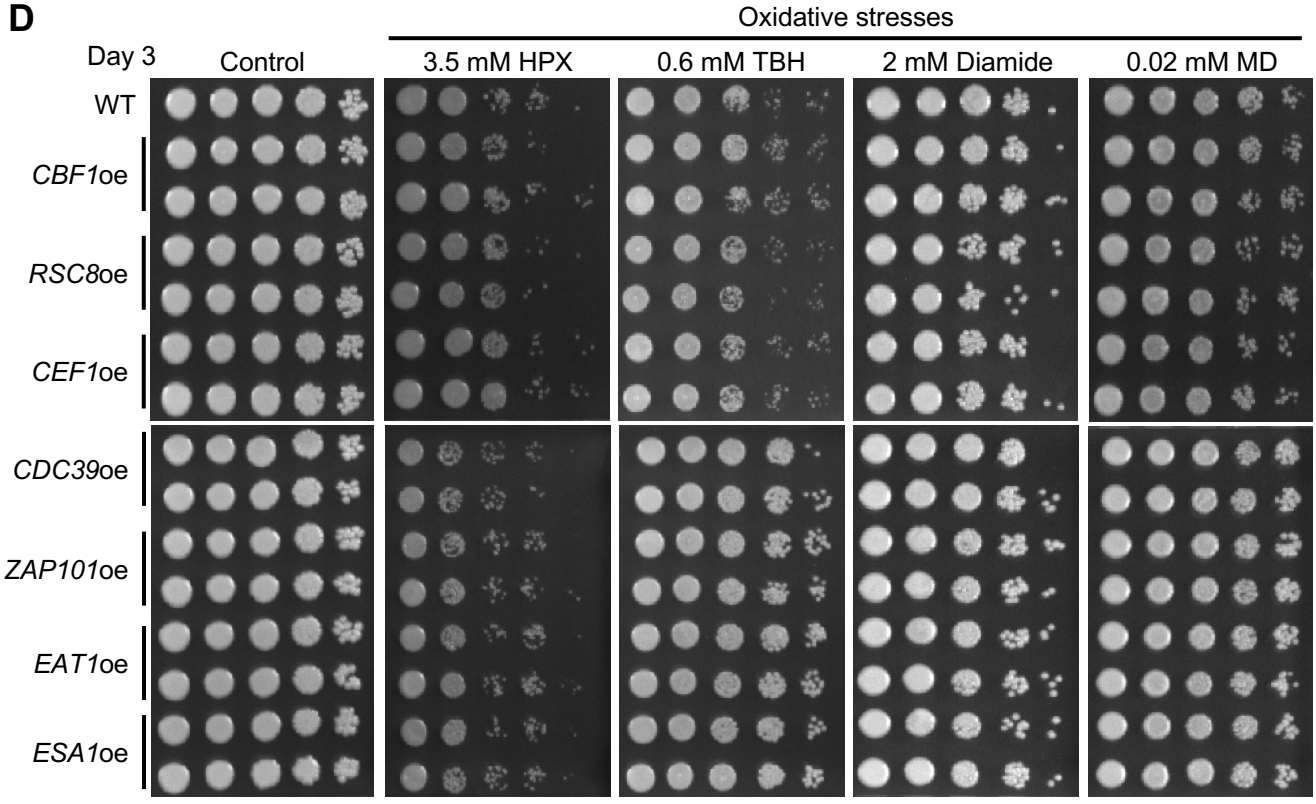
Oxidative stresses
Day 3
Control
3.5 mM HPX
0.6 mM TBH
2 mM Diamide
0.02 mM MD
WT
CBF1oe
RSC8oe
CEF1oe
CDC39oe
ZAP101oe
EAT1oe
ESA1oe

Continued

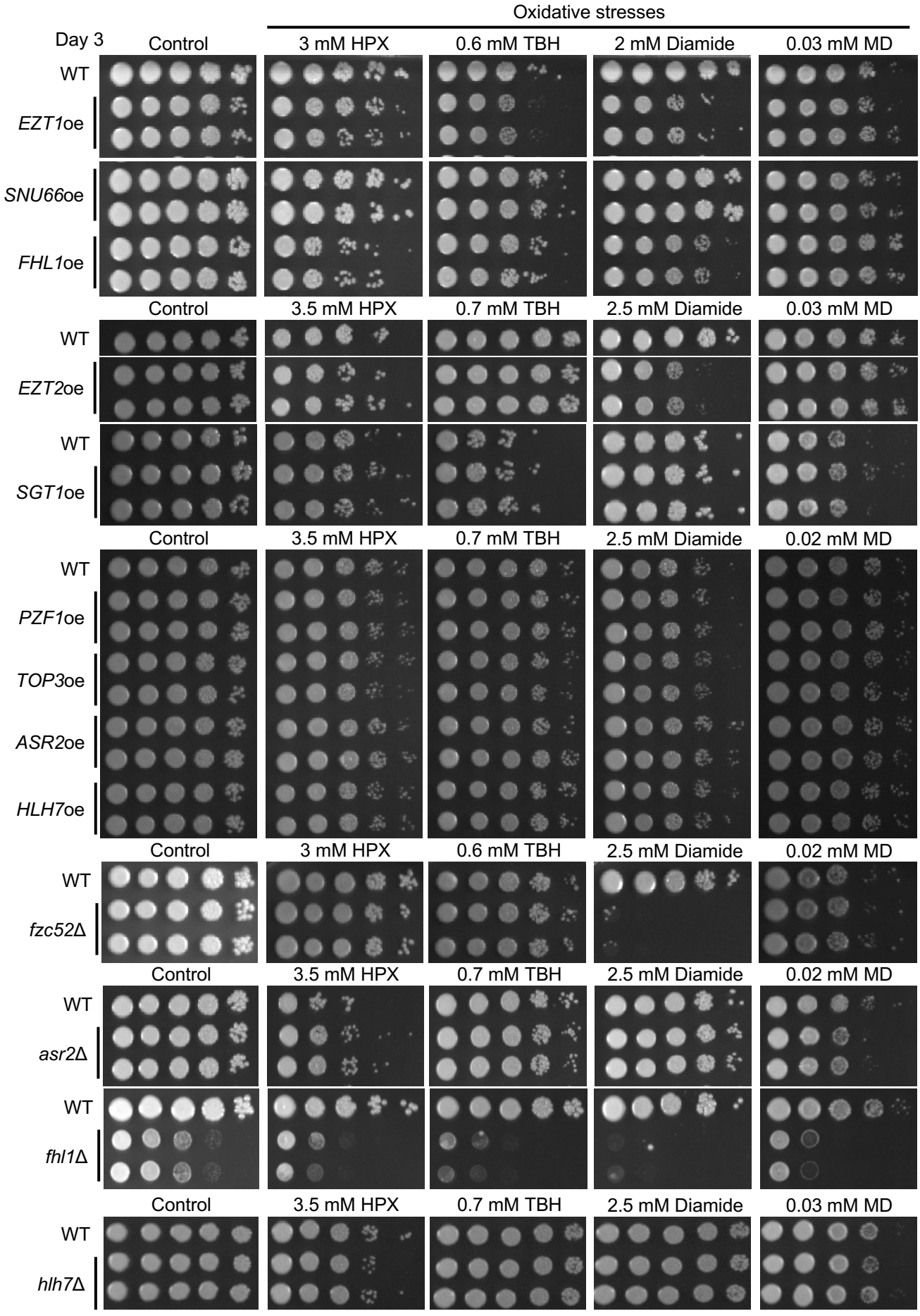
Oxidative stresses
Day 3
Control
3 mM HPX
0.6 mM TBH
2 mM Diamide
0.03 mM MD
WT
EZT1oe
SNU66oe
FHL1oe
Control
3.5 mM HPX
0.7 mM TBH
2.5 mM Diamide
0.03 mM MD
WT
EZT2oe
WT
SGT1oe
Control
3.5 mM HPX
0.7 mM TBH
2.5 mM Diamide
0.02 mM MD
WT
PZF1oe
TOP3oe
ASR2oe
HLH7oe
Control
3 mM HPX
0.6 mM TBH
2.5 mM Diamide
0.02 mM MD
WT
fzc52Δ
Control
3.5 mM HPX
0.7 mM TBH
2.5 mM Diamide
0.02 mM MD
WT
asr2Δ
WT
fhl1Δ
Control
3.5 mM HPX
0.7 mM TBH
2.5 mM Diamide
0.03 mM MD
WT
hlh7Δ

Continued

E

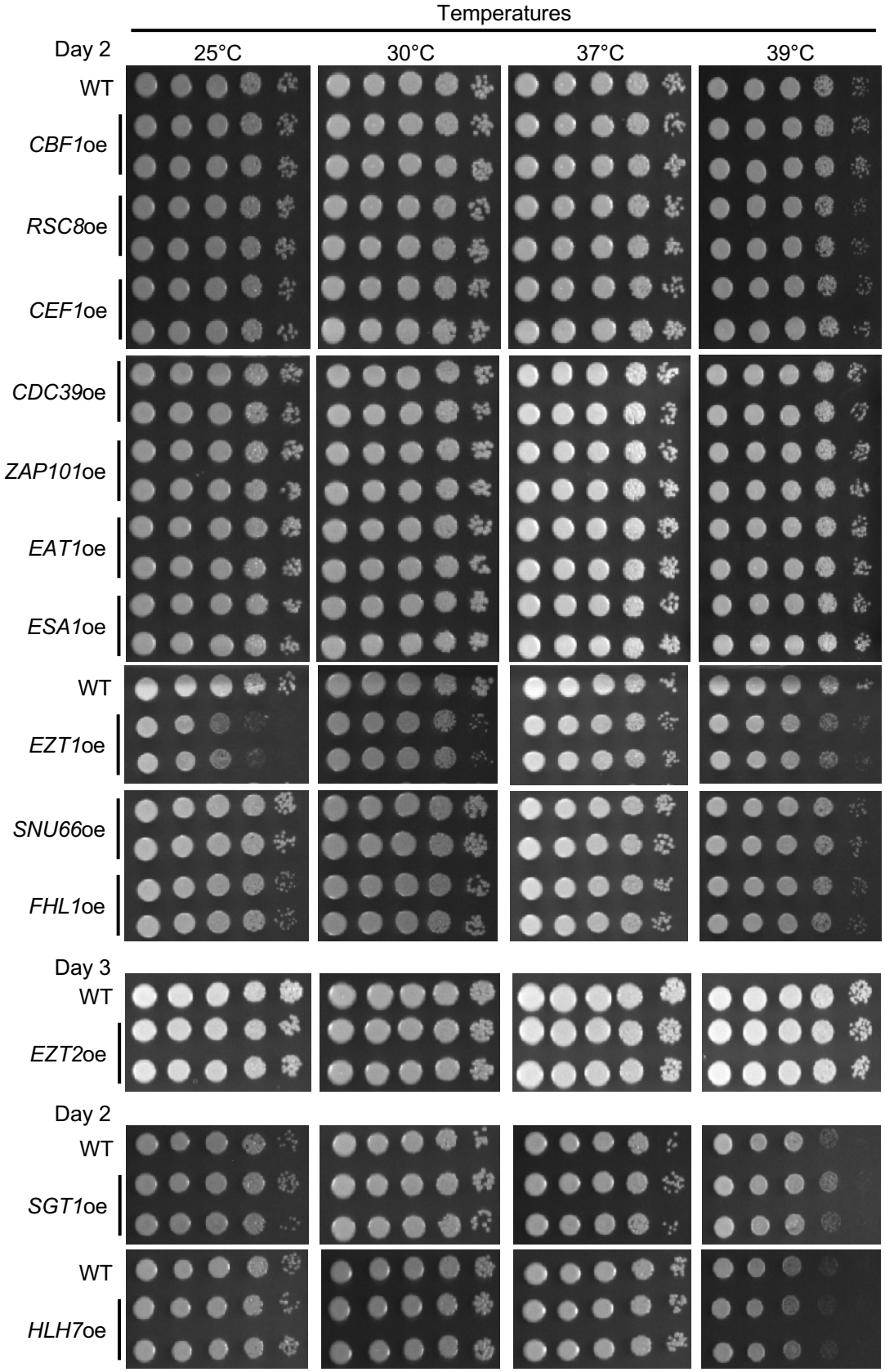
Temperatures
Day 2
25°C
30°C
37°C
39°C
WT
CBF1oe
RSC8oe
CEF1oe
CDC39oe
ZAP101oe
EAT1oe
ESA1oe
WT
EZT1oe
SNU66oe
FHL1oe
Day 3
WT
EZT2oe
Day 2
WT
SGT1oe
WT
HLH7oe

Continued

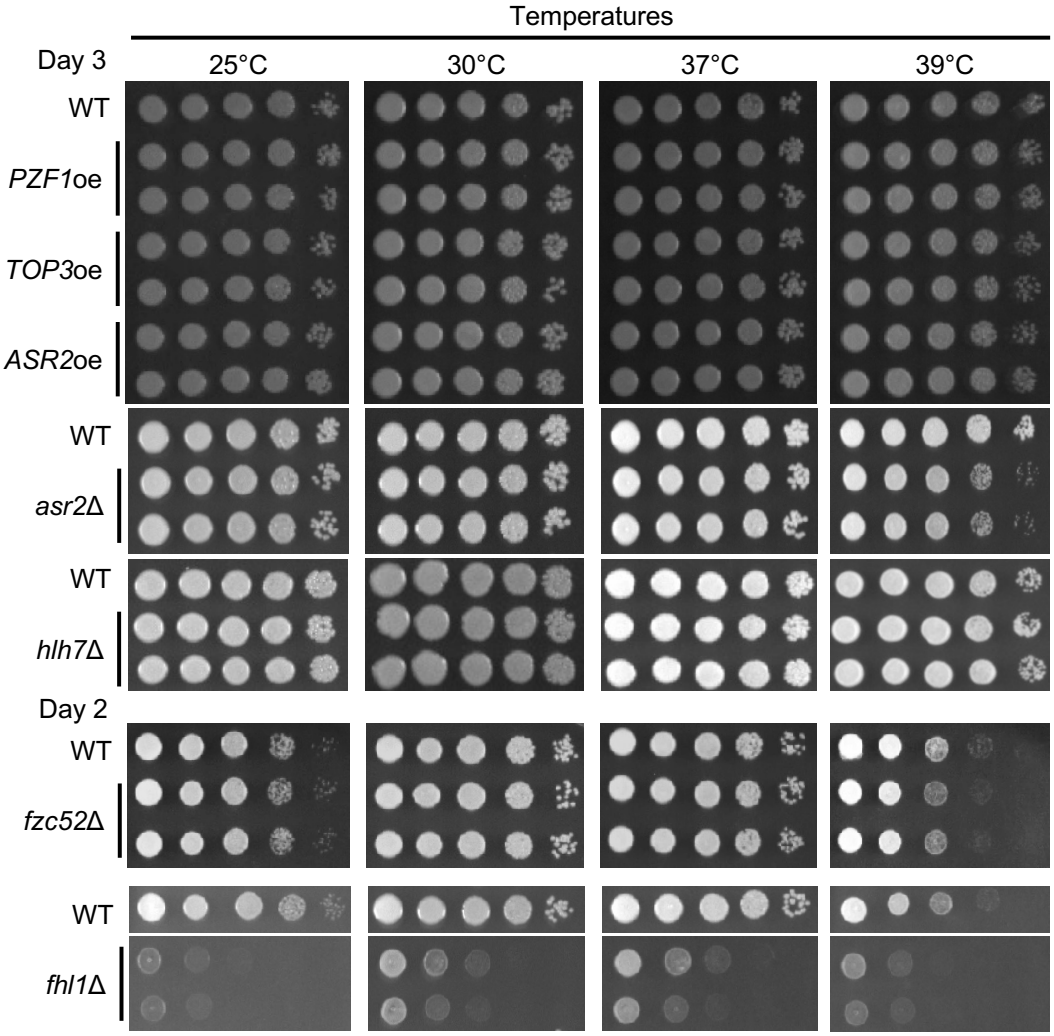
Temperatures
Day 3
25°C
30°C
37°C
39°C
WT
PZF1oe
TOP3oe
ASR2oe
WT
asr2Δ
WT
hlh7Δ
Day 2
WT
fzc52Δ
WT
fhl1Δ

F

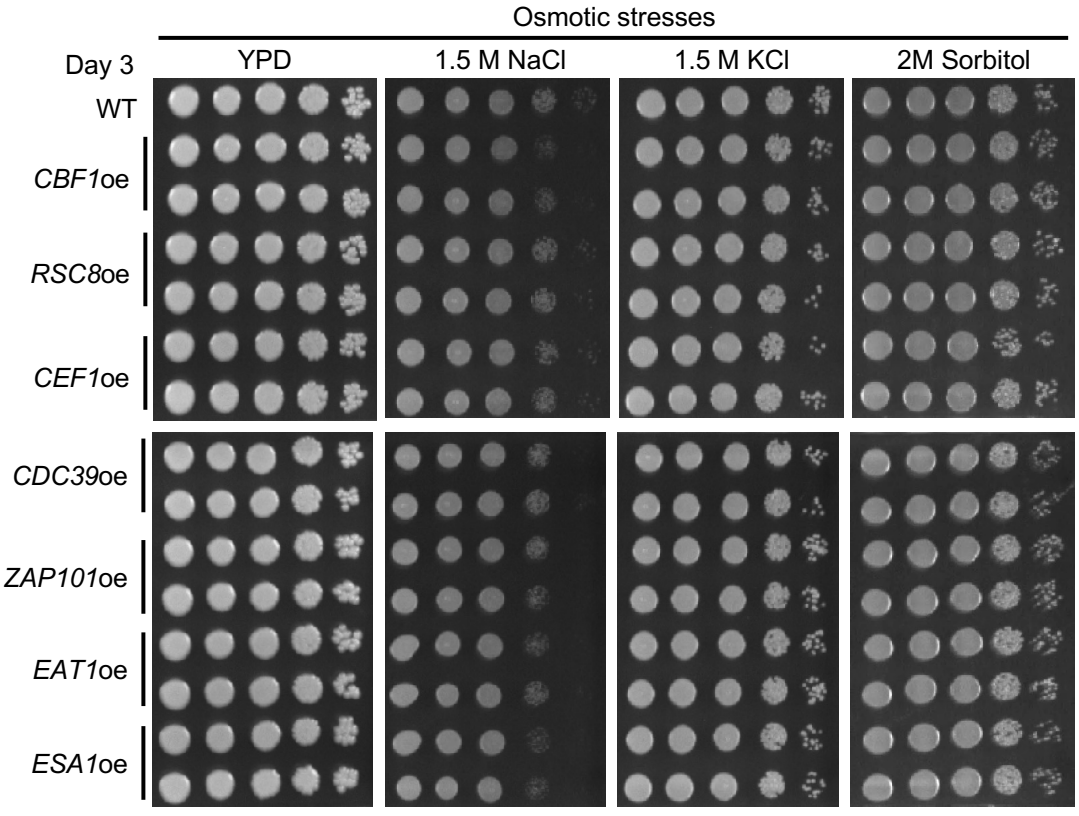
Osmotic stresses
Day 3
YPD
1.5 M NaCl
1.5 M KCl
2M Sorbitol
WT
CBF1oe
RSC8oe
CEF1oe
CDC39oe
ZAP101oe
EAT1oe
ESA1oe

Continued

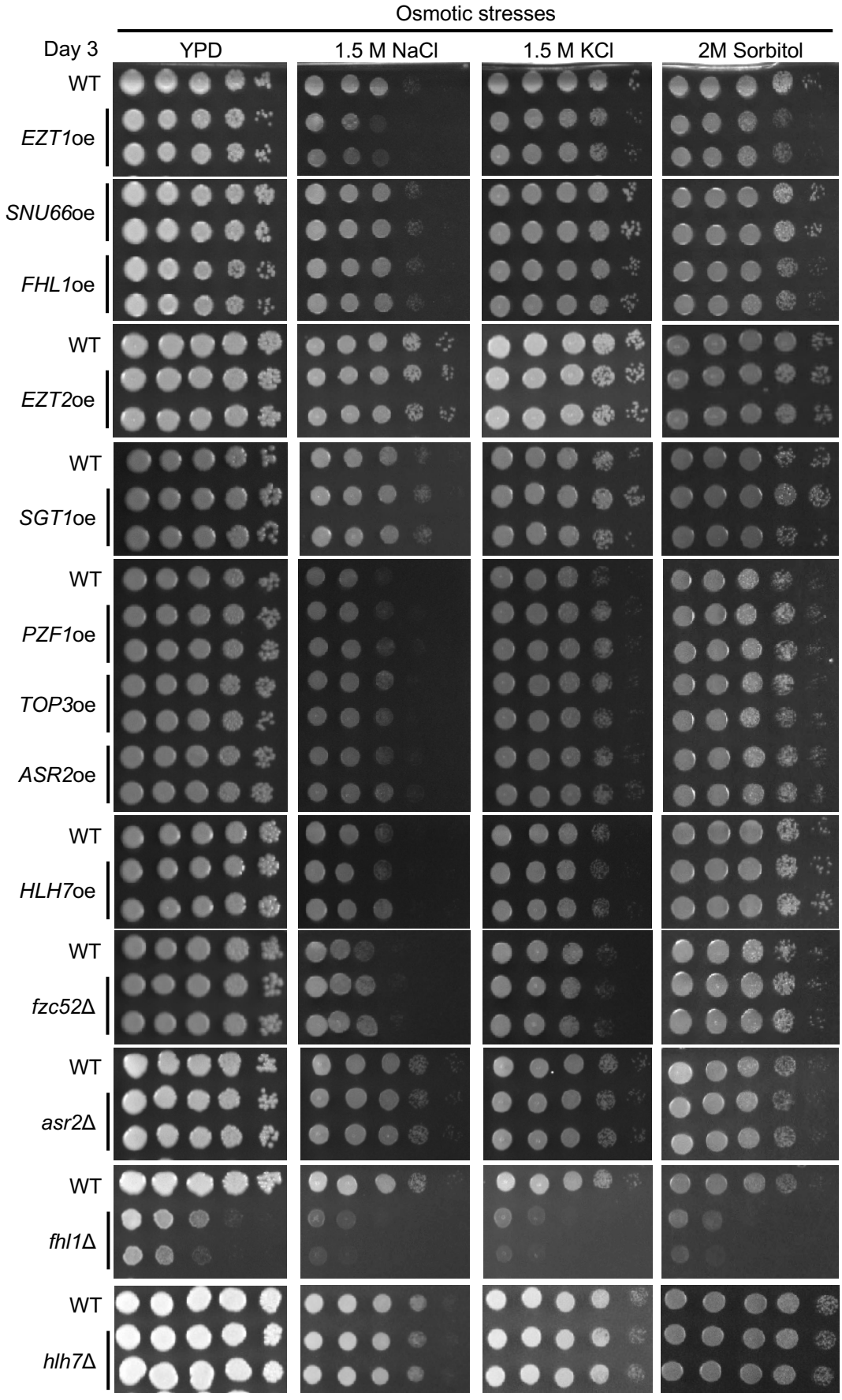
Osmotic stresses
Day 3
YPD
1.5 M NaCl
1.5 M KCl
2M Sorbitol
WT
EZT1oe
SNU66oe
FHL1oe
WT
EZT2oe
WT
SGT1oe
WT
PZF1oe
TOP3oe
ASR2oe
WT
HLH7oe
WT
fzc52Δ
WT
asr2Δ
WT
fhl1Δ
WT
hlh7Δ

Continued

G

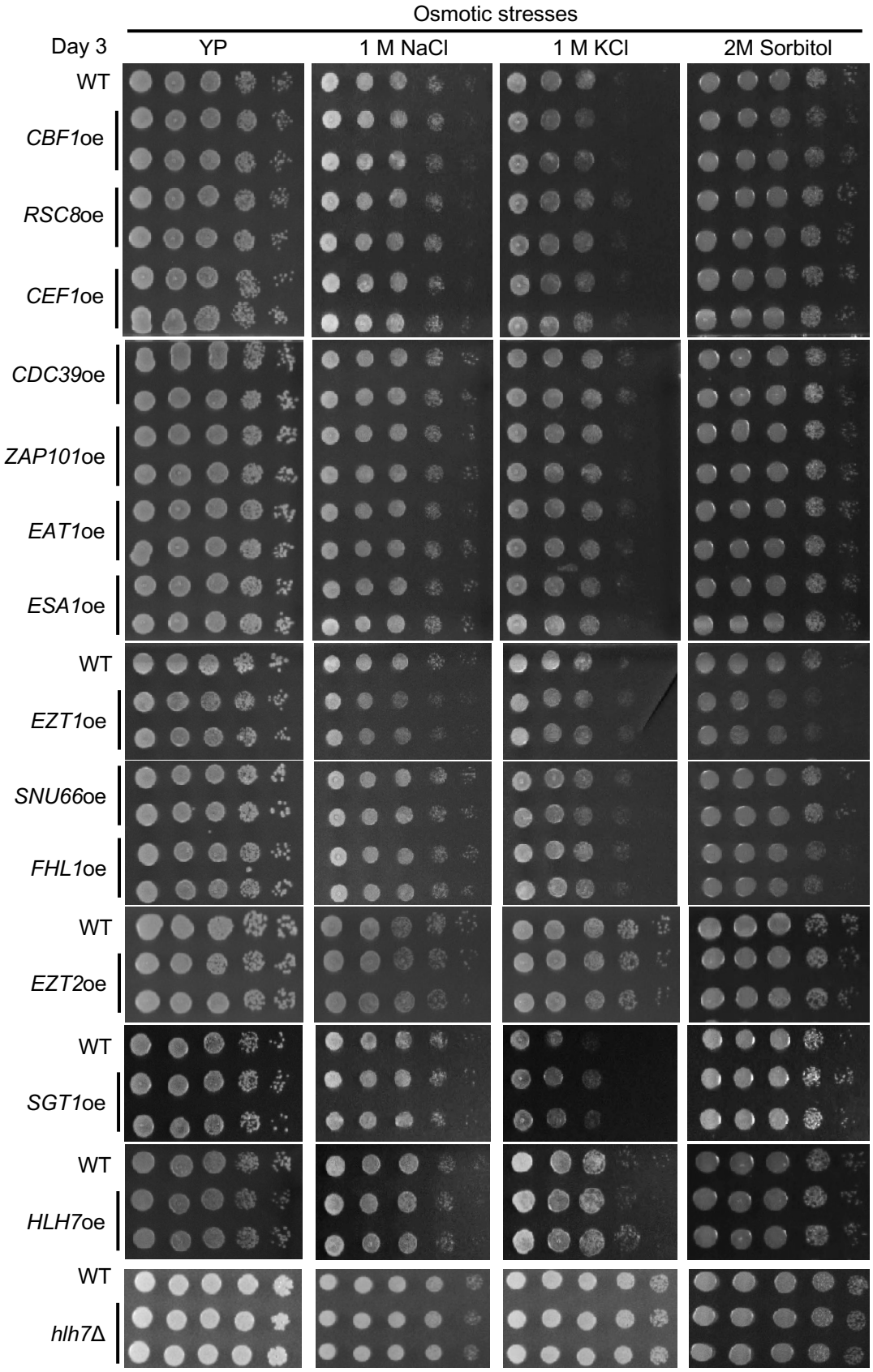
Osmotic stresses
Day 3
YP
1 M NaCl
1 M KCl
2M Sorbitol
WT
CBF1oe
RSC8oe
CEF1oe
CDC39oe
ZAP101oe
EAT1oe
ESA1oe
WT
EZT1oe
SNU66oe
FHL1oe
WT
EZT2oe
WT
SGT1oe
WT
HLH7oe
WT
hlh7Δ

Continued

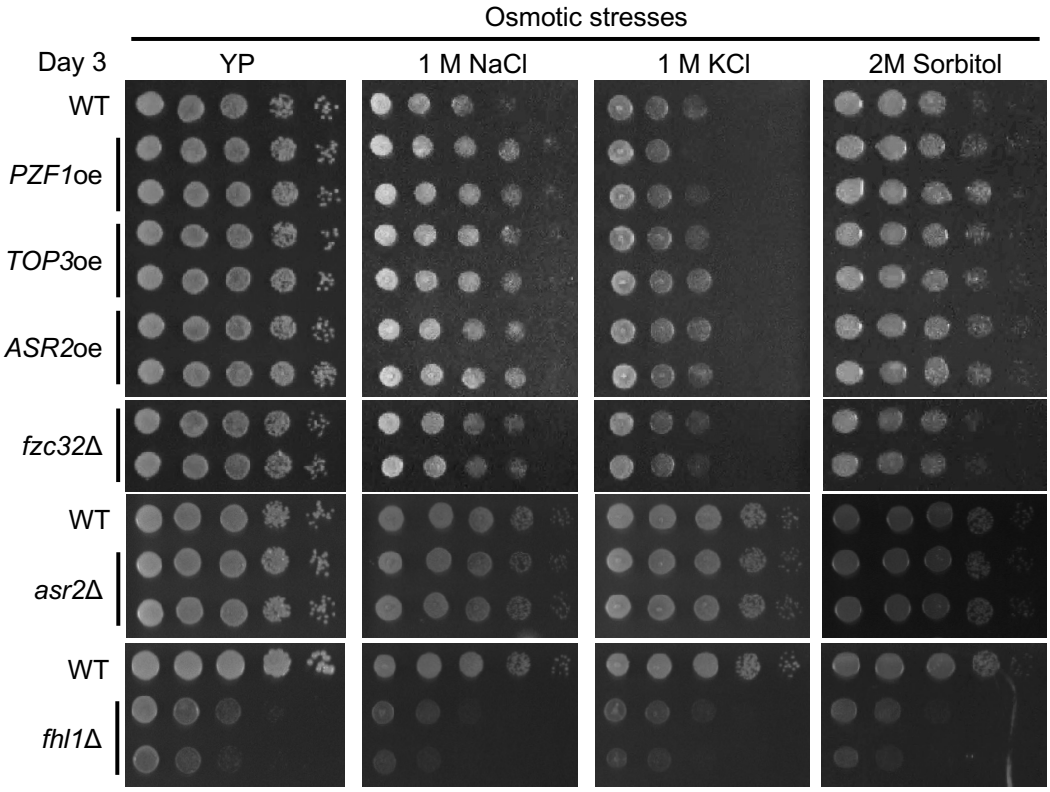
Osmotic stresses
Day 3
YP
1 M NaCl
1 M KCl
2M Sorbitol
WT
PZF1oe
TOP3oe
ASR2oe
fzc32Δ
WT
asr2Δ
WT
fhl1Δ

H

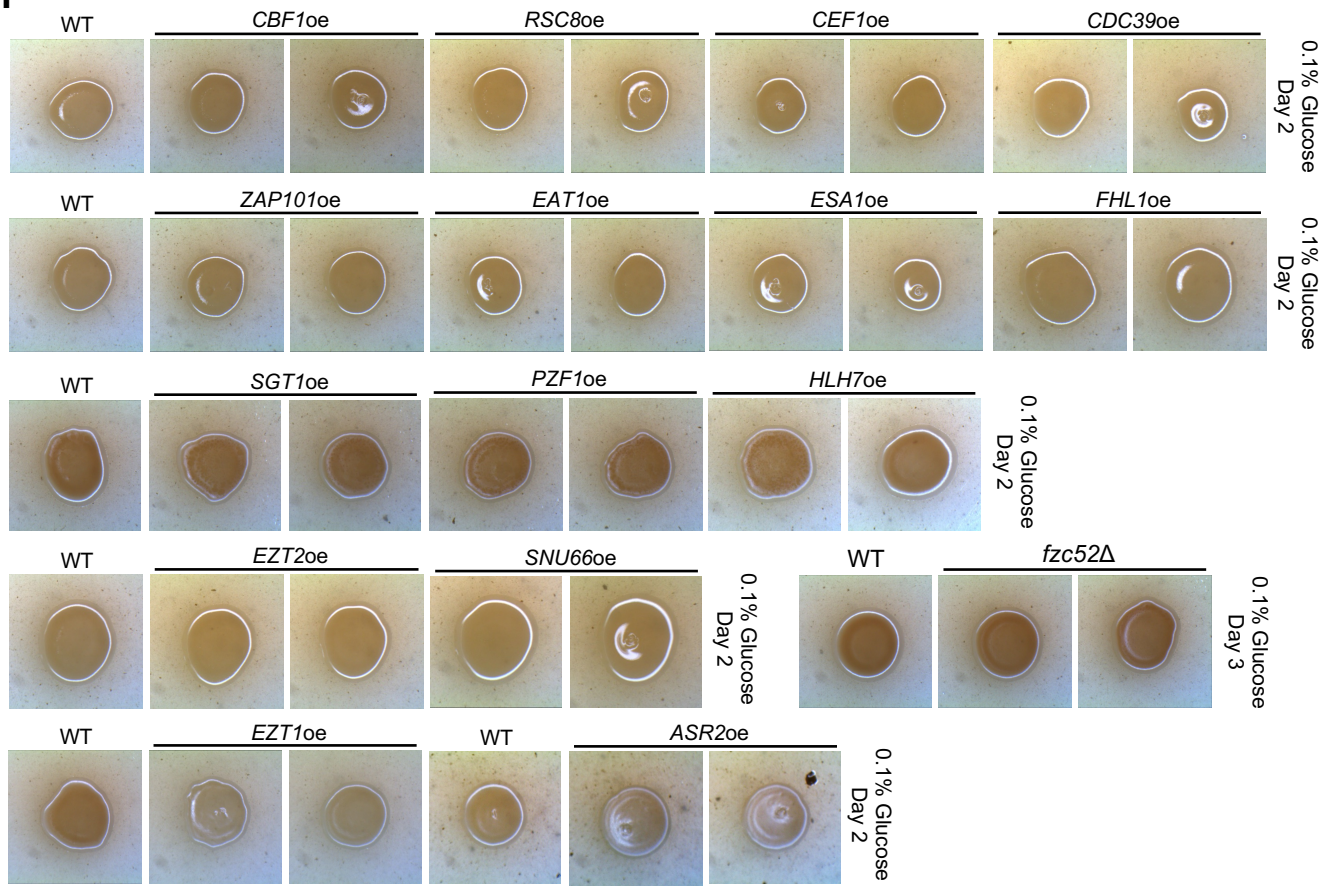
WT
CBF1oe
RSC8oe
CEF1oe
CDC39oe
0.1% Glucose Day 2
WT
ZAP101oe
EAT1oe
ESA1oe
FHL1oe
0.1% Glucose Day 2
WT
SGT1oe
PZF1oe
HLH7oe
0.1% Glucose Day 2
WT
EZT2oe
SNU66oe
0.1% Glucose Day 2
WT
fzc52Δ
0.1% Glucose Day 3
WT
EZT1oe
WT
ASR2oe
0.1% Glucose Day 2

Continued

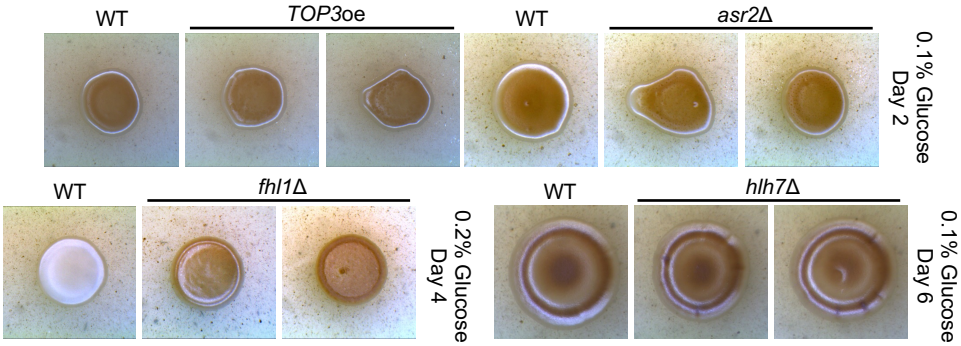

I

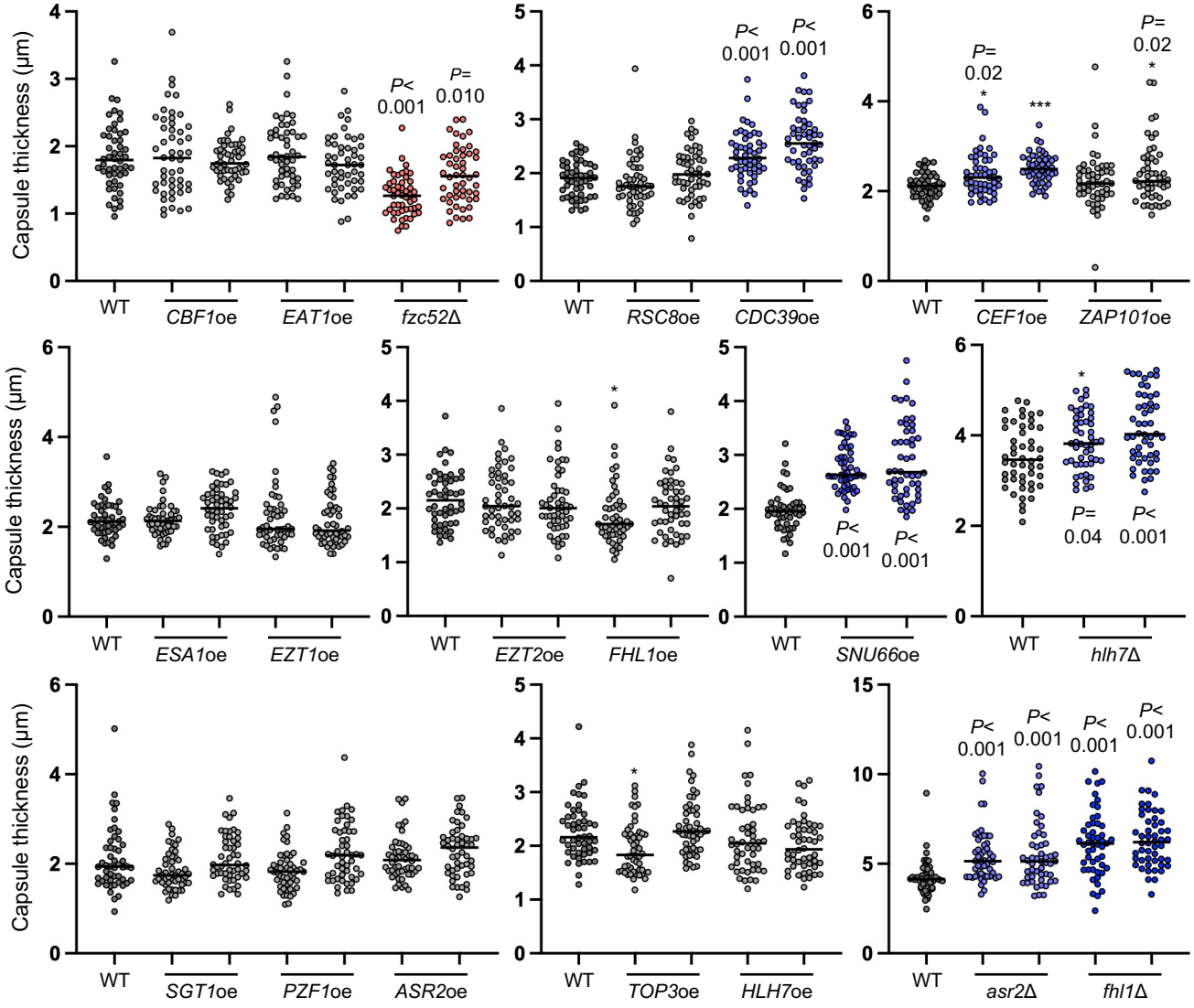

J

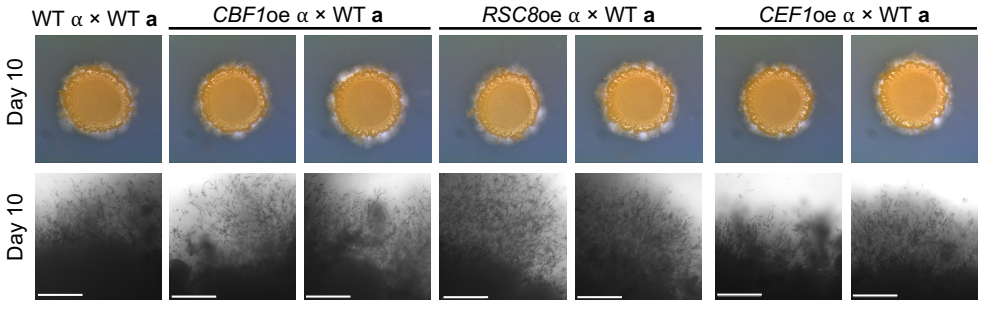

Continued

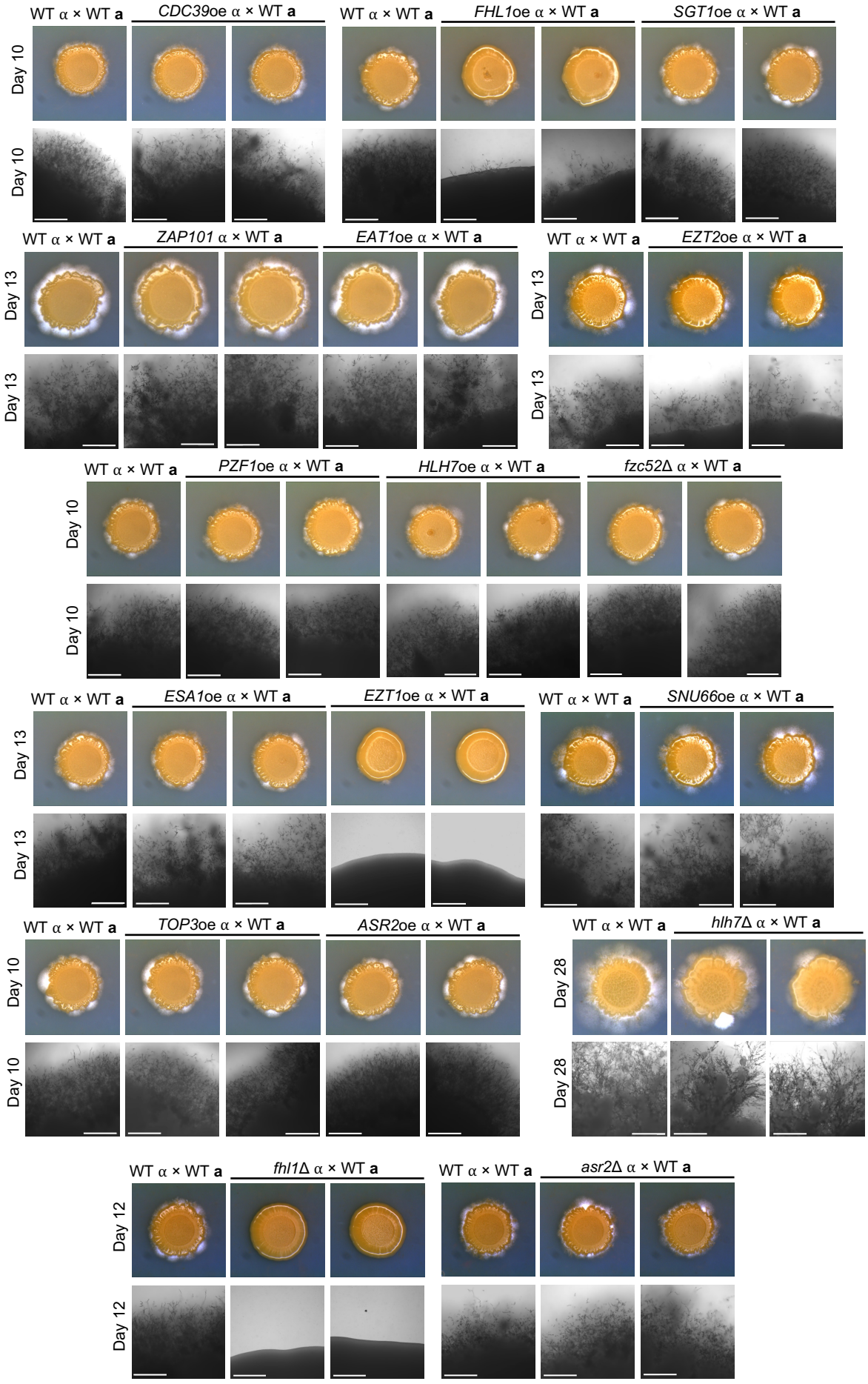

Figure legend is described on the next page.

Supplementary figure 8. Phenotypic analysis of the overexpression strains was conducted through various stress and antifungal drug treatments, virulence factor induction assays, and mating experiments. (A-G) The wild-type and the overexpression strains were cultured overnight at 30°C in liquid YPD medium, serially diluted (1 to 10^4), and spotted onto the YPD plates (3 µl) containing the indicated amount of stress or antifungal agents. Plates were incubated at 30°C (or designated temperature) and photographed after indicated days. (H and I) For virulence factor production assays, strains were grown in liquid YPD, washed twice with PBS, and 3 µl aliquots were spotted on 35 g/l Niger seed media with designated concentration of glucose (melanin induction assay) and DME media (capsule induction assays). Melanin induction was observed at 37°C and photographed at the indicated days with BX41 microscope (Olympus, Japan) with a SPOT digital camera (Diagnostic Instruments, Inc. USA). DME media plate was then incubated at 37°C for 2 days, and India ink staining was performed to visualise the capsules under a microscope. Capsule sizes were quantified by measuring both cell and capsule diameters using Nikon NIS software. Individual data points are shown, with the median indicated by a line. Statistical significances of differences between wild-type and the overexpression strain were determined by one-way ANOVA with Dunnett's multiple comparison test using Prism 11.0; *P* values are indicated above. (J) Mating filaments were observed after mating of the overexpression strains (*MAT*α) with wild-type YL99 *MAT* **a** and photographed at the indicated days using a differential interference contrast microscope ECLIPSE Ni (Nikon, Japan) equipped with DS-QI2 camera (scale bar: 400 µm) and BX51 microscope with a SPOT digital camera software. Each assay was repeated two or three times independently, and a representative image or dataset is shown here. Duplicated control images and data indicated that the same batch of wild-type and mutant strains were used in the indicated experiments and are presented here for comparison purposes.

Supplementary figure 9 (Lee et al.)

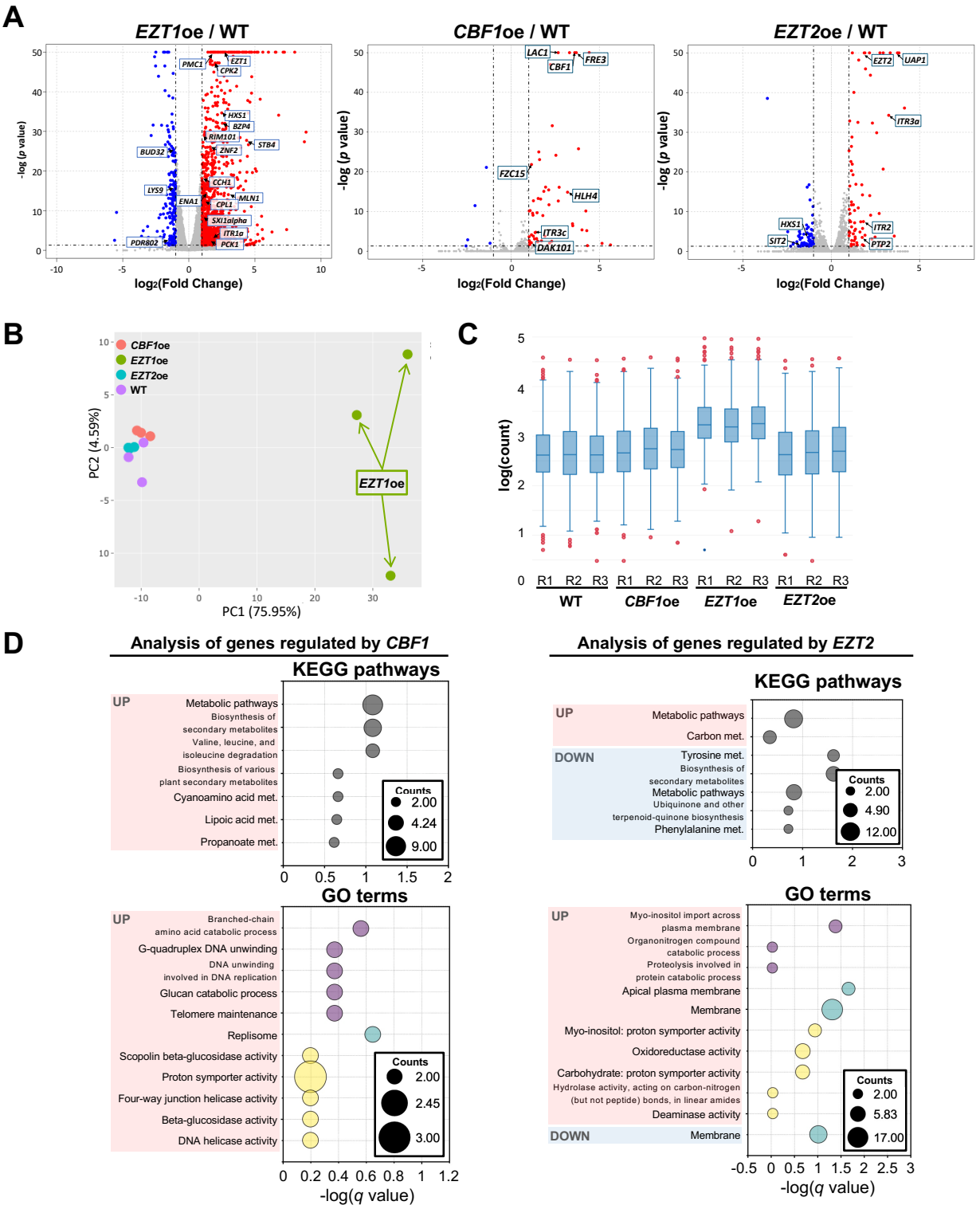

Supplementary figure 9. Transcriptome analysis of *CBF1*oe and *EZT2*oe. (A) Volcano plots showing differentially expressed genes (DEGs) in *EZT1*oe versus wild-type strains (left panel), *CBF1*oe versus wild-type strains (middle panel), and *EZT2*oe versus wild-type strains (right panel). The x-axis represents the $\log_2$ fold change (fc), and the y-axis represents the $-\log_{10}$(p-value). Genes with significant differential expression ($|\log_2 fc| > 1$ and p value < 0.05) are highlighted (red dots indicate upregulated genes, blue dots indicate downregulated genes, and gray dots indicate none-significant genes). (B) The principal component analysis (PCA) plot illustrating the extensive transcriptomic divergence caused by *EZT1*oe compared to *CBF1*oe and *EZT2*oe. (C) Interquartile range (IQR) analysis highlighting more pronounced transcriptomic changes in *EZT1*oe compared to the limited effects in *CBF1*oe and *EZT2*oe (R=biological replicate). (D) KEGG (Kyoto Encyclopedia of Genes and Genomes) analysis and GO (Gene Ontology) term analysis of the significantly regulated genes by the overexpression of *CBF1* (left panel) and *EZT2* (right panel) identified significantly overrepresented biological processes and regulated metabolic and signalling pathways.

Supplementary figure 10 (Lee et al.)

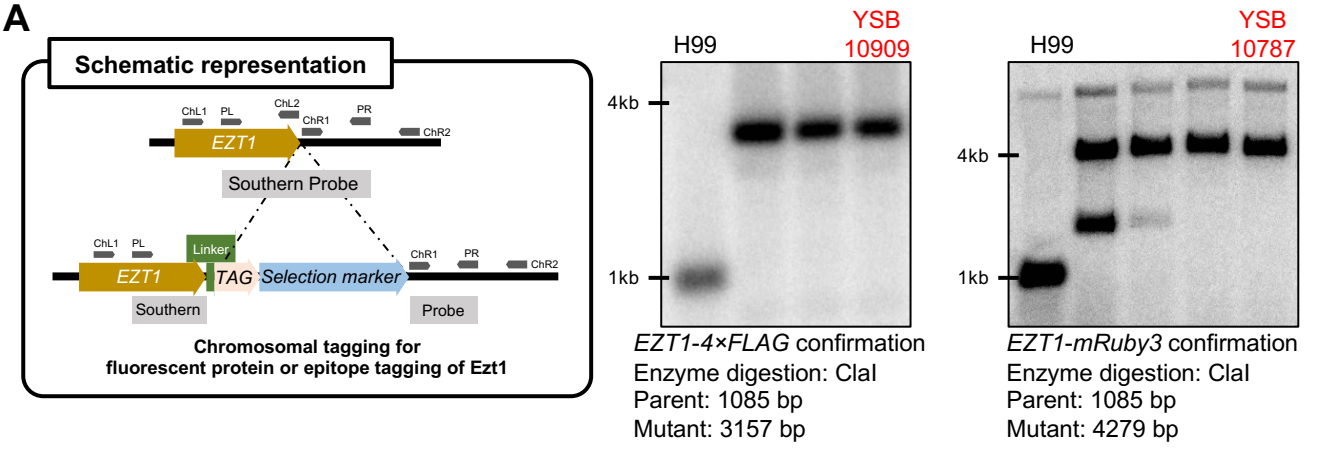

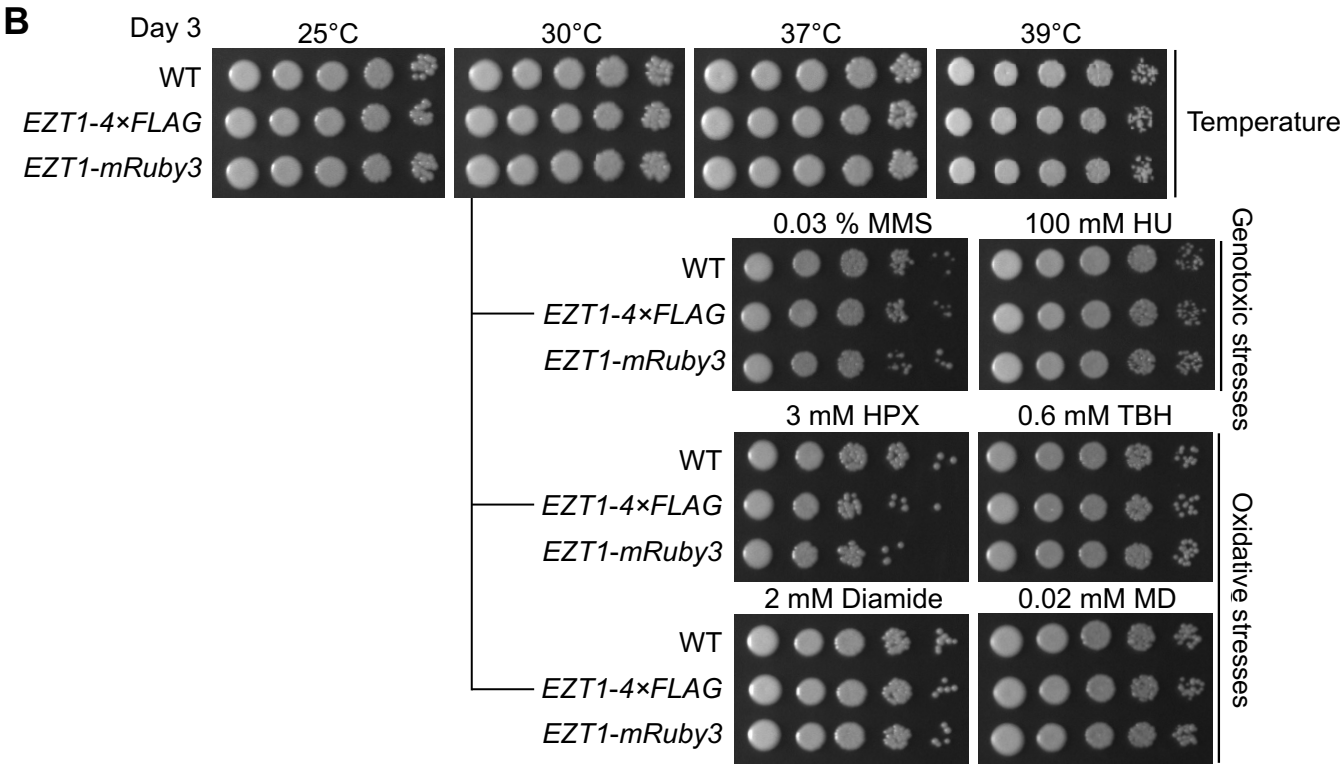

Continued

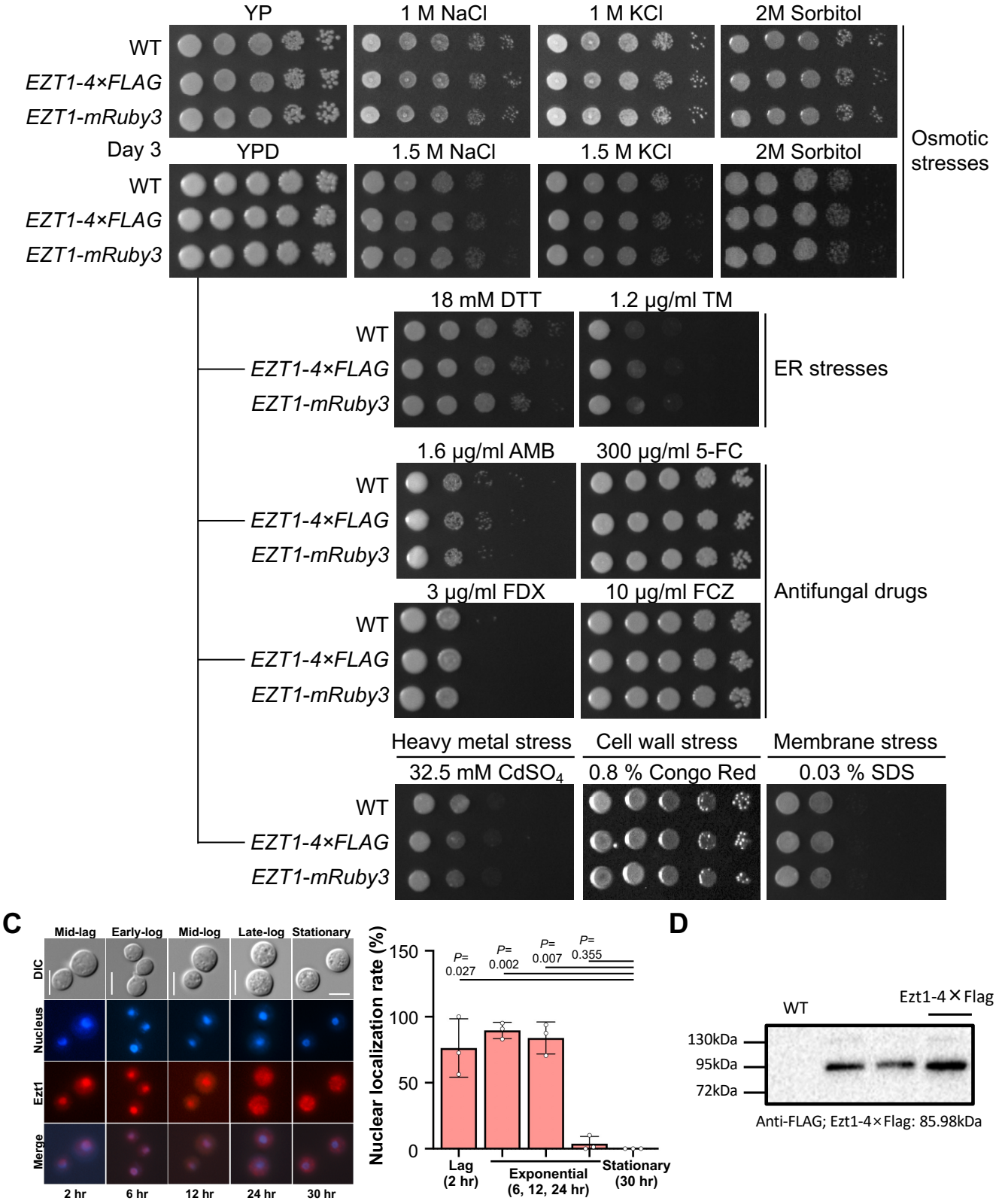

Supplementary figure 10. Chromosomal tagging of Ezt1. (A) Schematic representation for the construction of Ezt1-4×FLAG and Ezt1-mRuby3 strains is shown in box. Correct genotypes of the strains were confirmed through Southern blot analysis with the restriction enzyme ClaI and *EZT1*-specific probe. (B) The functional validation of Ezt1 proteins tagged with FLAG and mRuby3 was conducted through phenotypic analysis. The wild-type and the chromosomally tagged strains were cultured overnight at 30°C in liquid YPD medium, serially diluted (1 to 10^4), and spotted onto the YPD plates (3 μl) containing the indicated amount of stress or antifungal agents. Plates were incubated at 30°C (or designated temperature) and photographed after 3 days. (C) Cellular localization of Ezt1. Fluorescence microscopy showed nuclear localisation of Ezt1-mRuby3 during the exponential growth phase, with cytoplasmic translocation occurring from the late-log to stationary phases (scale bar: 5 μm). Data are represented as mean ± SD. Statistical significance of difference was determined by one-sample *t*-test using Prism 11.0 (*P* values are stated above). (D) Detection of the Ezt1-4×FLAG protein through Western blot analysis. The wild-type and *EZT1-4×FLAG* strains were cultured in YPD medium at 30°C, synchronized to OD_{600nm}=0.2, and grown to OD_{600nm}=0.8. Cells were harvested, frozen in liquid nitrogen, and lysed using bead beating in lysis buffer (50mM Tris-HCl [pH 7.5], 1% sodium deoxycholate, 5 mM sodium pyrophosphate, 0.1 μM sodium orthovanadate, 50mM NaF, 0.1% SDS, 1% Triton X-100, 0.5 μM PMSF, and 1×protease inhibitor cocktail). After centrifugation, proteins were separated via SDS-PAGE, transferred to PVDF membrane, and probed with anti-FLAG (1:2000) antibody. Detection was performed using HRP-conjugated secondary antibody and ECL chemiluminescence, followed by imaging with a ChemiDoc XRS+ system (Biorad, USA).

Supplementary figure 11 (Lee et al.)

A

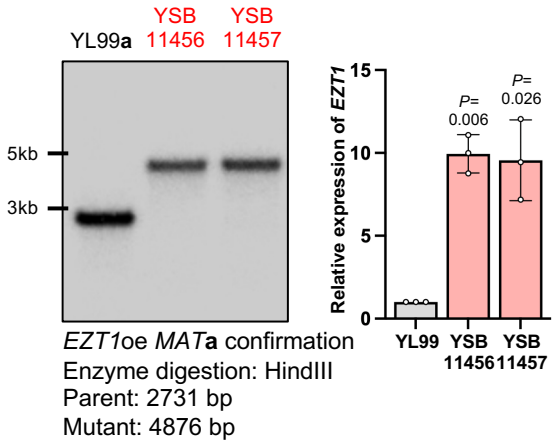

*EZT1*oe *MAT***a** confirmation
Enzyme digestion: HindIII
Parent: 2731 bp
Mutant: 4876 bp

B

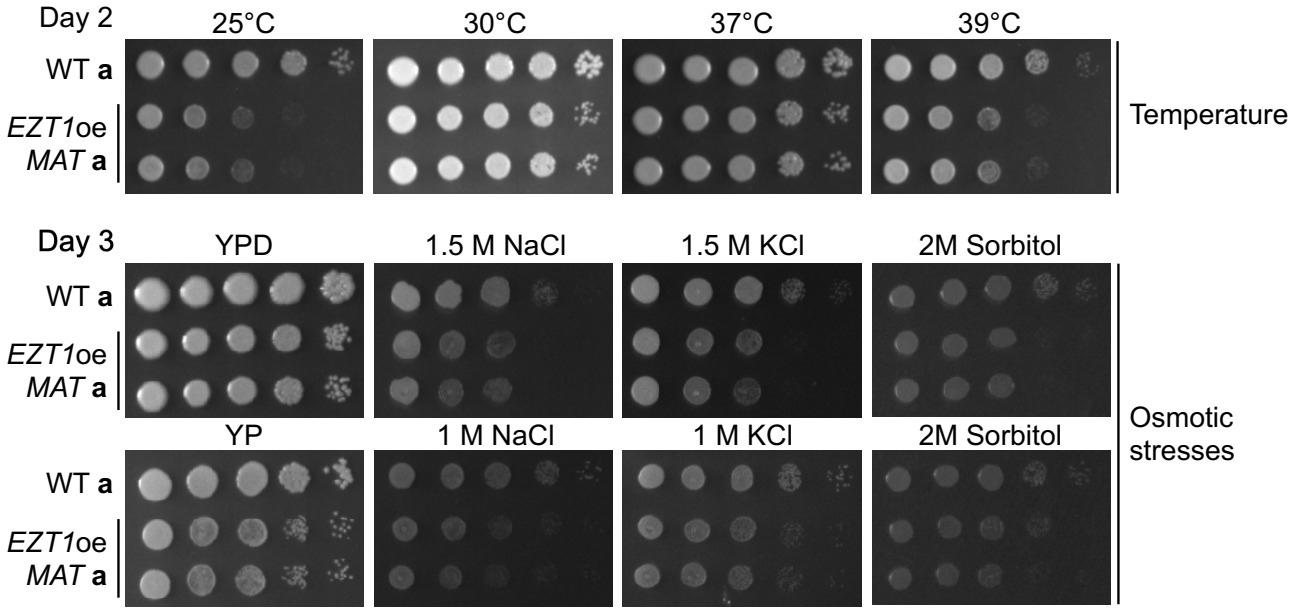

Continued

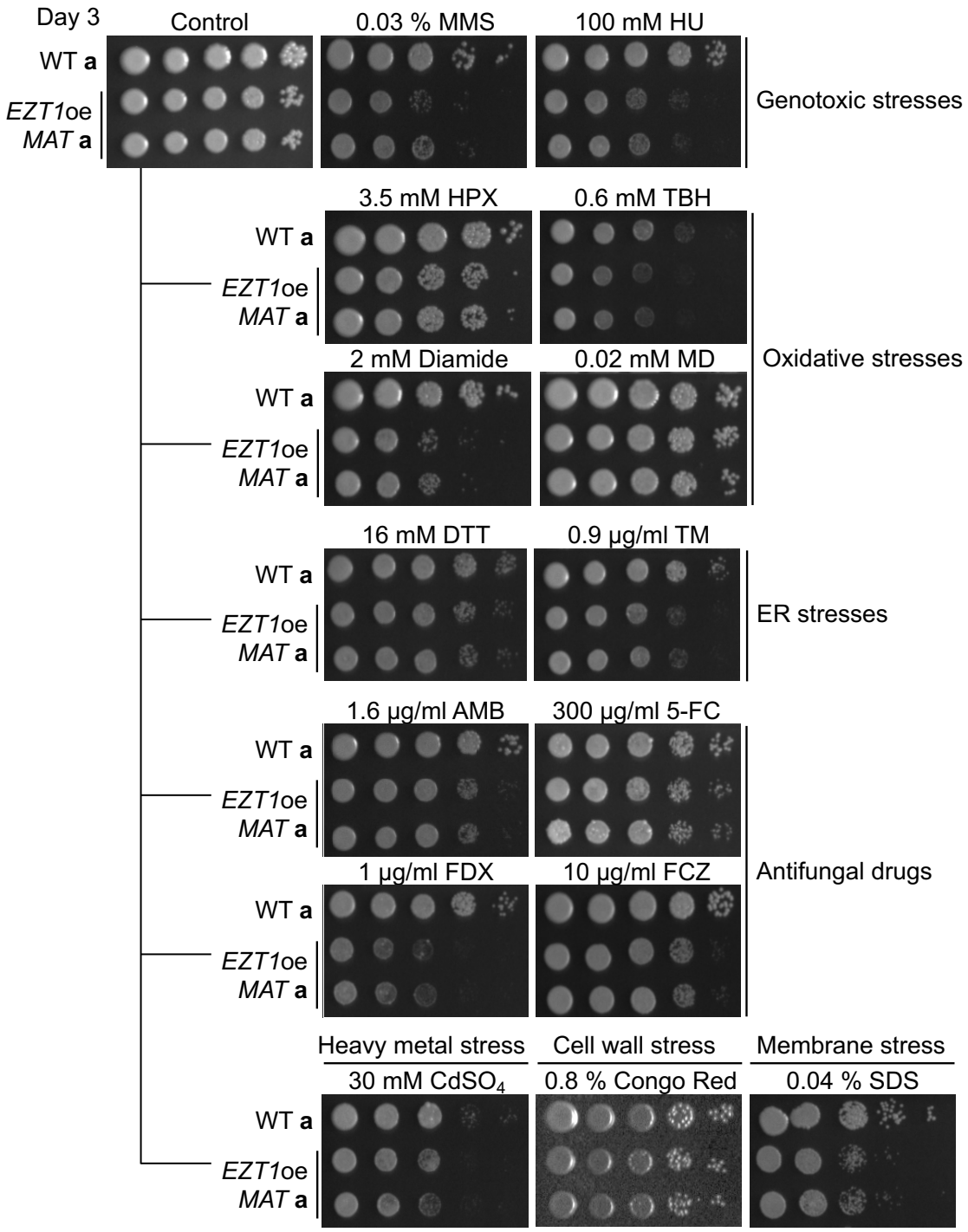

Supplementary figure 11. The *MAT*a *EZT1*oe strain phenocopied the *MAT*α *EZT1*oe strain. (A) The correct genotype of the *MAT***a** *EZT1*oe strains was confirmed through Southern blot analysis with the restriction enzyme HindIII and *EZT1*-specific probe. The overexpression of the targeted genes was confirmed with qRT-PCR using the identical procedure as for the expression validation of the essential TF overexpression strains. Data are represented as mean ± SD. Statistical significances of differences between wild-type and the overexpression strain were determined by one-sample *t*-test using Prism 11.0 (*P* values are stated above). (B) The phenotypic analysis confirmed that *EZT1*oe *MAT* **a** and *EZT1*oe *MAT* α exhibit the same phenotype. The wild-type and the overexpression strains were cultured overnight at 30°C in liquid YPD medium, serially diluted (1 to 10^4), and spotted onto the YPD plates (3 μl) containing the indicated amount of stress or antifungal agents. Plates were incubated at 30°C (or designated temperature) and photographed after designated days.

Supplementary figure 12 (Lee et al.)

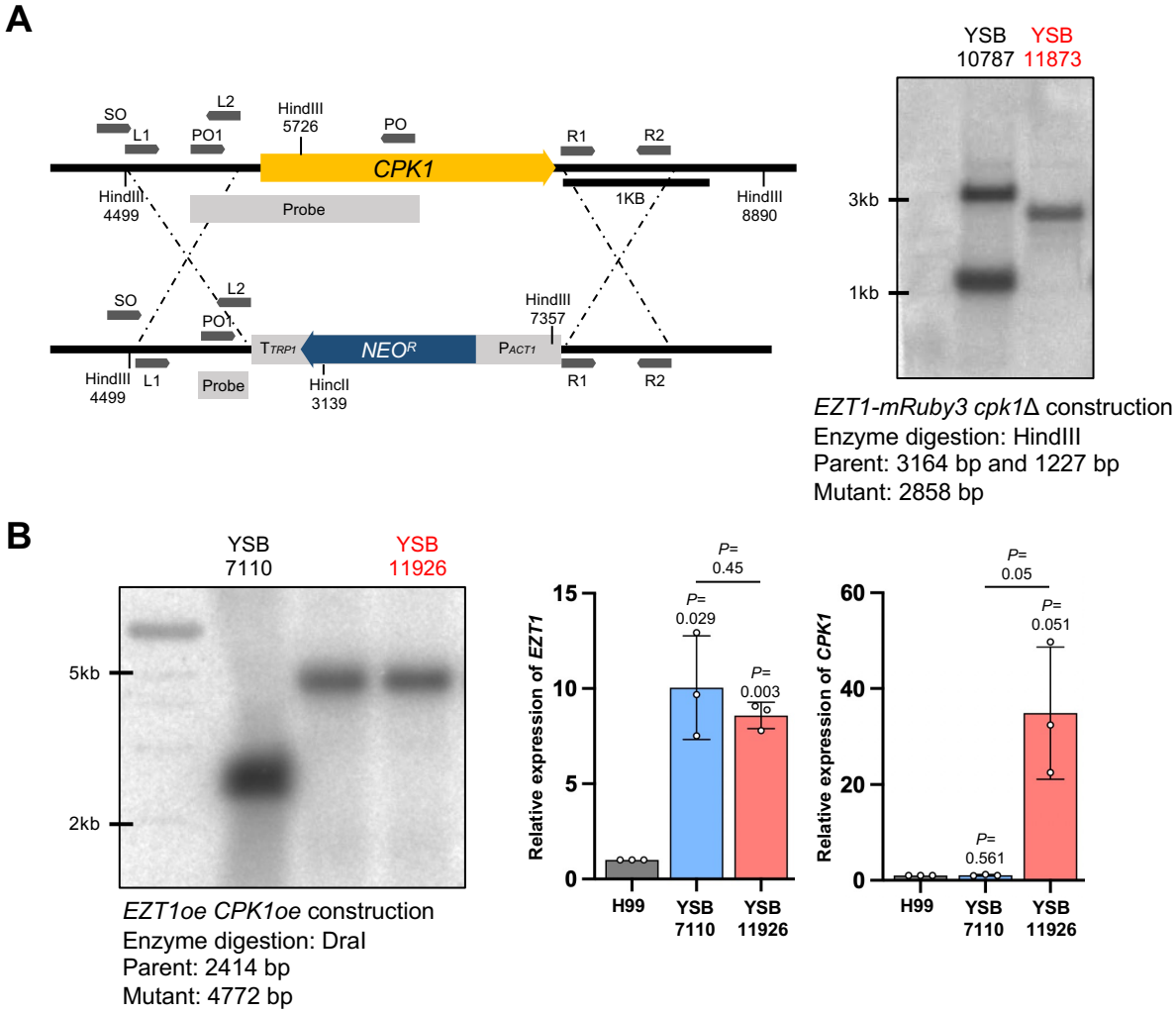

Supplementary figure 12. Construction of strains to investigate the relationship between *EZT1* and *CPK1*. (A) Strategy and confirmation of the constructed *EZT1*-mRuby3 *cpk1*Δ strain. Southern blot analysis confirmed the genotype of the constructed mutant with the restriction enzyme HindIII digestion. (B) Correct genotype of the *EZT1* and *CPK1* double overexpression strain was confirmed through Southern blot analysis with the restriction enzyme DraI and *CPK1*-specific probe. The overexpression of the targeted genes was confirmed with qRT-PCR using the identical procedure as for the expression validation of the essential TF overexpression strains. Data are represented as mean ± SD. Statistical significances of differences were determined by one-sample *t*-test for the overexpression and unpaired *t*-test between *EZT1*oe and *EZT1*oe *CPK1*oe using Prism 11.0 (*P* values are indicated above).

Supplementary figure 13 (Lee et al.)

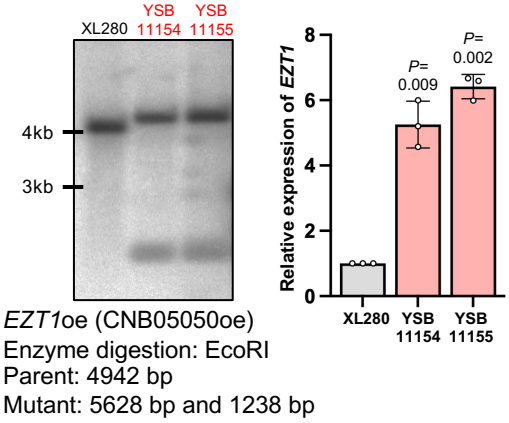

Supplementary figure 13. Construction of *EZT1* overexpression strains in XL280. (A) Correct genotype of the *Cryptococcus deneoformans EZT1* (CNB05050) overexpression strains was confirmed through Southern blot analysis with the restriction enzyme HindIII and *EZT1*-specific probe. The overexpression of the targeted genes was confirmed with qRT-PCR using the identical procedure as for the expression validation of the essential TF overexpression strains. Data are represented as mean ± SD. Statistical significances of differences between wild-type and the overexpression strains were determined by one-sample *t*-test compared to the wild-type for the overexpression strains using Prism 10.0 (*P* values are indicated above)

Supplementary figure 14 (Lee et al.)

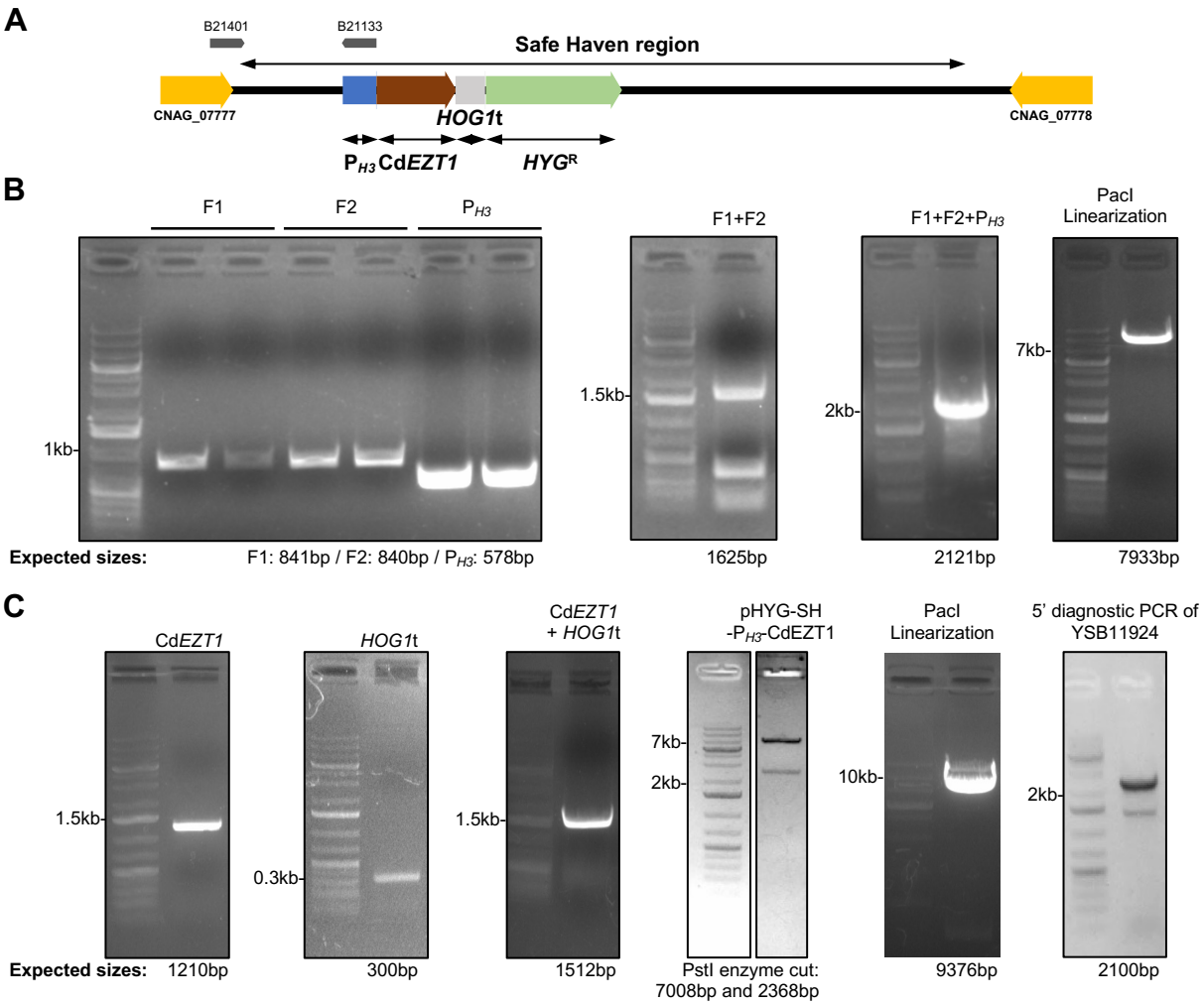

Supplementary figure 14. Heterologous expression of *Cryptococcus depauperatus EZT1*. (A) Schematic strategy for constructing a strain heterologously overexpressing *Cryptococcus depauperatus EZT1* (Cd*EZT1*). (B) To construct the pHYG-SH(Safe Haven)-P$_{H3}$-Cd*EZT1* plasmid, the intergenic region between CNAG_00777 and CNAG_00778 was divided into two fragments (F1 and F2) and amplified by PCR. These fragments were then fused through overlap PCR to introduce AscI, BaeI, and PacI restriction sites in the middle of the intergenic region. Subsequently, the *H3* promoter (P$_{H3}$) was amplified and integrated with the intergenic region via overlap PCR. This fused fragment was ligated with pHYG using Gibson assembly (New England Biolabs, USA), resulting in the pHYG-SH-P$_{H3}$ plasmid (confirmed with PacI linearization). (C) To introduce Cd*EZT1*, the L203_03018 gene from *C. depauperatus* CBS7841 was PCR-amplified and assembled into pHYG-SH-P$_{H3}$ using Gibson assembly, yielding the final pHYG-SH-P$_{H3}$ -Cd*EZT1* plasmid (confirmed with Pst1 enzyme digestion). The plasmid was linearized by PacI digestion, and the purified cassette was subsequently introduced into the P$_{CTR4}$:*EZT1* strain. Transformant is confirmed with 5' junctional diagnostic PCR.